

ADA023135

18 19 6 9
FUNDAMENTAL RESEARCH IN
EXPLOSIVE MAGNETOHYDRODYNAMICS.

9 Final Report. 1 Oct 74-31 Dec 75

AFOSR Contract No. F44629-75-C-0017

15 Recd
By Malcolm S. Jones, Jr.

10

Contract Monitor
Dr. B. T. Wolfson

AF-9752

975242

16

17

11 Feb 1976

12 84 p.



Malcolm Jones Associates, Inc.
P. O. Box 67
Corona del Mar, California 92625

Telephone: (714) 673-7473

Approved for public release; distribution unlimited

AIR FORCE OFFICE OF SCIENTIFIC RESEARCH (AFSC)
NOTICE OF EXECUTION OF LOGO
This logo is a registered trademark and is
used to denote that the document has been reviewed and is
distributed in accordance with AFSC AFM 190-12 (7b).
A. D. WESSE
Technical Information Officer

Best Available Copy



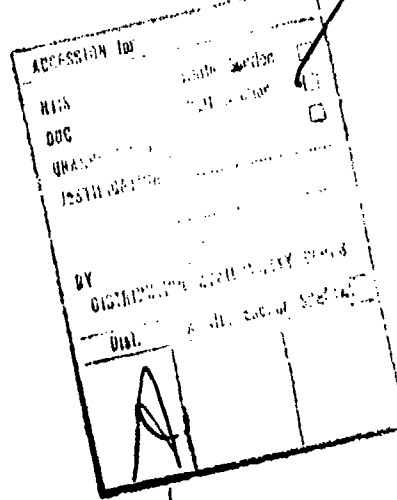
341684

1.B

Qualified requestors may obtain additional copies from the Defense Documentation Center; all others should apply to the National Technical Information Service.

Conditions of Reproduction

Reproduction, translation, publication, use and disposal in whole or in part by or for the United States Government is permitted.



FUNDAMENTAL RESEARCH IN EXPLOSIVE MAGNETOHYDRODYNAMICS

TABLE OF CONTENTS

	<u>PAGE</u>
ABSTRACT	vi
ACKNOWLEDGEMENTS	viii
1.0 INTRODUCTION	1
2.0 REVIEW OF EXPLOSIVE DRIVEN MHD POWER GENERATION	3
2.1 EXPLOSIVE DRIVEN MHD GENERATOR DESCRIPTION	3
2.2 ELECTRICAL PARAMETERS	3
2.2.1 Initial Magnetic Induction B_0	3
2.2.2 Pulse Lengths	5
2.2.3 Generator Size	5
2.2.4 Generator Load	5
2.3 GASDYNAMIC PARAMETERS	5
2.4 EXPLOSIVE PARAMETERS	6
2.5 SEEDING PARAMETERS	6
2.6 MAJOR PROBLEM AREAS	6
3.0 ANALYTICAL STUDIES ON EXPLOSIVE DRIVEN MHD GENERATORS . . .	8
3.1 REVIEW OF PREVIOUS DATA	8
3.1.1 The Role of Shock-Heating in the Explosive Driven MHD Generator	8
3.1.2 Bulk Seeded Explosives	14
3.2 CIRCUIT ANALYSIS	21
4.0 SCALE-UP OF EXPLOSIVE DRIVEN MHD GENERATORS	29
4.1 5MJ DESIGN STUDY	29
4.2 30MJ EXPLOSIVE DRIVEN MHD ASSEMBLY	32
4.3 SEEDED DETONATION PRODUCT FAST SWITCH	35
4.4 HERCULES SCALE-UP EXPERIMENT	41
APPENDIX A	42
A.1 AVCO-Shock Hydrodynamics-Atlantic Research Program . .	42
A.2 The Hercules, Inc., Program	47
REFERENCES	73

LIST OF FIGURES

	<u>PAGE</u>
Figure 2.1 GENERALIZED MHD GENERATOR CIRCUIT	4
Figure 3.1 PEAK CURRENT IN EXPLOSIVE DRIVEN MHD GENERATOR AS A FUNCTION OF PRESSURE OF HELIUM OR ARGON ORIGINALLY IN CHANNEL FOR VARIOUS LOAD RESISTANCES	10
Figure 3.2 TIME OF PEAK CURRENT AND TIME CURRENT STARTS TO DROP SHARPLY AS A FUNCTION OF INITIAL PRESSURE OF ARGON OR HELIUM IN CHANNEL OF EXPLOSIVE DRIVEN MHD GENERATOR	12
Figure 3.3 VARIATION OF PEAK CURRENT AS A FUNCTION OF INITIAL PRESSURE OF ARGON OR HELIUM IN THE CHANNEL FOR VARIOUS RESISTIVE LOADS	13
Figure 3.4 VOLTAGE CURRENT CURVES FOR BULK SEED PBX CHARGES. ALSO SHOWN IS DATA FOR RDX CHARGE SURFACE SEEDED WITH 200 Mg CESIUM PICRATE	16
Figure 3.5 PEAK CURRENT IN EXPLOSIVE DRIVEN MHD GENERATOR AS A FUNCTION OF MASS OF Cs PICRATE SURFACE SEEDED USED WITH BULK SEEDED PBX CHARGES AND UNSEEDED RDX CHARGES	18
Figure 3.6 VARIATION IN SHORT-CIRCUITED GENERATOR CURRENT DECAY TIME, τ , FOR BULK SEEDED PBX CHARGES AND UNSEEDED RDX CHARGES AS A FUNCTION OF MASS OF CESIUM PICRATE SURFACE SEEDED	20
Figure 3.7 TIME-SPACE DIAGRAM FOR THE MOVEMENT OF PLASMA IN A MAGNETIC FIELD AND CURRENT DENSITY DISTRIBUTION; A-I-FRONT OF A REFRACTED WAVE; 2-FRONT OF LUMINESCENCE; 3-BOUNDARY OF THE NONELECTROCONDUCTIVE ZONE; B-1-12 MICROSECONDS FROM THE START OF THE CURRENT; 2-24; 3-36; 4-48; 5-60; 6-72; 7-84.	24
Figure 4.1 METHOD OF INTERCONNECTING EXPLOSIVE DRIVEN MHD CHANNEL TO INCREASE GENERATOR INTERNAL RESISTANCE	30
Figure 4.2 METHOD OF CONNECTING BACK-TO-BACK EXPLOSIVE DRIVEN MHD CHANNELS TO INCREASE GENERATOR IMPEDANCE EXPLOSIVE CHARGE E SHOULD BE INITIATED AT POINT A	30
Figure 4.3 DETAILS OF EXPLOSIVE DRIVEN MHD GENERATOR TO PRODUCE 5MJ PULSES, 100 MICROSECONDS IN DURATION.	33
Figure 4.4 CONCEPTUAL DESIGN OF 30MJ EXPLOSIVE DRIVEN MHD GENERATOR	34
Figure 4.5 EXPLOSIVE MHD SWITCH CONFIGURATION AT END OF COAXIAL LINE	38
Figure 4.6 PREDICTED VOLTAGE RECOVERY CURVE	40
Figure A.1 OSCILLOGRAMS OF TWO SETS OF TRANSVERSE ELECTRODE VOLTAGES AND CURRENTS FROM AVCO TEST NO. 13	44
Figure A.2 HERCULES X-MHD CHANNEL SCHEMATIC WITH MAGNETIC FIELD PROFILE AND PHOTOGRAPH	51
Figure A.3 OSCILLOSCOPE TRACES FOR HERCULES SHOT X-MHD 1	54

	<u>PAGE</u>
Figure A.4 ANALYSIS OF HERCULES SHOT X-MHD 1	55
Figure A.5 OSCILLOSCOPE TRACES FOR HERCULES SHOT X-MHD 2 . . .	56
Figure A.6 OSCILLOSCOPE TRACES FOR HERCULES SHOT X-MHD 9 . . .	58
Figure A.7 VOLTAGE-CURRENT PLOT FOR THE WEST (DRIVEN) CHANNEL IN HERCULES SHOT X-MHD 6	61
Figure A.8 VOLTAGE-CURRENT TRAJECTORIES FOR THE WEST CHANNEL IN SHOT X-MHD 13	64
Figure A.9 VOLTAGE-CURRENT TRAJECTORIES FOR THE WEST CHANNEL ON HERCULES SHOT X-MHD 14	65
Figure A.10 VOLTAGE-CURRENT TRAJECTORIES FOR HERCULES SHOT X-MHD 15	66
Figure A.11 CURRENT-VOLTAGE TRAJECTORY FOR HERCULES SHOT X-MHD 16	67
Figure A.12 VOLTAGE-CURRENT TRAJECTORIES FOR HERCULES SHOT X-MHD 19	68
Figure A.13 SUMMARY OF PEAK CURRENT DATA FOR THE DRIVER CHANNEL IN THE HERCULES EXPERIMENTS	70
Figure A.14 SUMMARY OF PEAK CURRENT DATA FOR THE DRIVEN CHANNEL IN THE HERCULES EXPERIMENTS	71

LIST OF TABLES

	<u>PAGE</u>
Table III-1 DATA FROM TEST IN 1" x 4" EXPLOSIVE DRIVEN MHD GENERATOR USING HELIUM AND ARGON AT VARIOUS PRESSURES AS THE INITIAL FILLING GAS.	9
Table III-2 CURRENT DECAY TIME CONSTANTS FOR BULK SEEDED CHARGES IN 1" x 4" EXPLOSIVE DRIVEN MHD GENERATOR	15
Table A-1 DATA FROM AVCO CONDUCTIVITY TESTS	46
Table A-2 SUMMARY OF HERCULES TEST DATA	52
Table A-3 OPEN-CIRCUIT SHOT ANALYSIS	59
Table A-4 EFFECT LOAD RESISTANCES - MILLIOHMS	63

ABSTRACT

The background experimental work with explosive driven MHD generators is reviewed and the major parametric factors are outlined. Previously unpublished data on the effects of the density and composition of gases originally in the channel is reviewed and it is shown that the major conduction path is through the seeded detonation products and that the role of the gas is secondary. Unpublished data on experiments with bulk seeded charges is also presented. It is shown that RDX charges surface seeded with more than 100 mg of cesium picrate produced better results than any of the bulk seeded charges tested, which contained up to 25% CsNO_3 . A deleterious interaction was observed when bulk seeded charges were surface seeded with cesium picrate. Analysis of this data also revealed that the anomalously high internal inductance of the explosive driven MHD generator was reduced by increasing the seed level, meaning that the seed effects both the plasma conductivity and inductance.

The effect of various circulating current systems on the explosive derived plasma slug are examined. It is determined that diamagnetic surface currents coupled with a thermal ionization instability producing a "T-layer" can be responsible for the maintenance of the plasma conductivity in the generator. However, such a mechanism cannot be responsible for the initial conductivity observed in the vicinity of the explosive charge in the absence of a magnetic field. The physical basis for this original conductivity is uncertain. ↗

To demonstrate the need for more data on explosive driven MHD generators, designs are presented for three interesting applications: 5 MJ 100 microsecond pulses into a 1 ohm load; 30 MJ pulses 700 microseconds long into 3006 20 ohm flash lamps; and a coaxial switch for fast capacitor banks. The major uncertainty is the maximum duration of the pulse which can be produced by an explosive driven MHD channel.

The work on two recent Air Force sponsored programs in explosive MHD is reviewed. It is concluded that the data taken under Contract F33615-72-C-1395 does not substantiate the claim that the measured conductivity of the seeded detonation products was between 625 and 1250 mho/m, or that the gas conductivity increased with increasing seed level from 1% to 5%. The theoretical work under Contract F33615-72-C-1394 is questionable; however, the experimental work under

that program using back-to-back channels facing a single explosive charge is viewed as making an important contribution to the explosive driven MHD generator technology.

ACKNOWLEDGEMENTS

We would like to thank Dr. B. T. (Terry) Wolfson for having the courage to sponsor this work at a time when explosive MHD was in disfavor with the U.S. Air Force and treated with a ho-hum attitude by most of the rest of the U.S. Government agencies.

We would especially like to thank C. Bangerter and B. Hopkins of Hercules, Inc., for making their soon to be published data available to us for analysis. If our analysis of their data seems harsh, i.e., concluding data channels were reversed, etc., these are honest investigator-to-investigator communications which demonstrate the difficulties of explosive MHD experimentation; with this report as the vehicle to cover the intervening thousands of miles and no criticism is intended.

We would like to thank Prof. A. E. Sheindlin of the Moscow High Temperature Institute for making certain papers on explosive driven MHD progress in the Soviet Union available to us. Regretably, the limited time available under this study did not allow us to make a detailed analysis of their extensive analytical and experimental work on the subject. We would also like to thank Dr. E. F. Lebedev of the High Temperature Institute for pointing out to us the applicability of the T-layer concept to the explosive driven MHD generator.

Mostly we thank L. M. Rogers for his assistance in the preparation of the manuscript.

The contributions of all of these people to the success of this work is gratefully acknowledged by the author.

FUNDAMENTAL RESEARCH IN
EXPLOSIVE MAGNETOHYDRODYNAMICS

1.0 INTRODUCTION

For about fifteen years we have known that by passing the detonation products from a seeded explosive charge through a magnetic field that short intense pulses of electricity could be produced. From the very beginning it was clear that the conventional laws or receipes for describing the conductivity of dense, low temperature plasmas were not applicable to the high-pressure seeded detonation products. Early measurements {1,3} showed that the conductivity was about 1000 mho/m which is about two orders of magnitude too high for thermal equilibrium ionization of low ionization potential materials such as cesium or potassium at chemical explosion temperatures.

In an effort to gain some understanding of this conduction mechanism we conducted a wide variety of experiments in channels of different shapes; used different explosive compositions; changed the chemical and physical properties of gases surrounding the explosive charge and filling the channel; and tested a variety of low ionization potential seeded materials in various chemical compositions (1-7). While we still do not have a clear theoretical picture of the basic conductivity mechanism at higher pressures we do know that the successful operation of the explosive driven MHD generator depends intimately upon what happens to the seed material on the face of the explosive charge and that it is this explosive derived plasma that provides the dominant portion of the interaction with the magnetic field in the MHD channel.

In preparing this report we have had three goals:

a. To summarize previous work on explosive MHD in one place so that those who are willing to follow an Edisonian approach can take the available data and design explosive driven MHD generators to produce pulses of the size and shapes they desire with a high-level of confidence that these devices will perform as designed. Why try to re-invent the wheel or develop elaborate new theories?

b. To summarize recent work by others and to determine whether these results contribute to the understanding of the fundamental problems in explosive MHD, and

c. To clearly outline the fundamental problems and suggest areas where answers may be found.

To illustrate the magnitude of the problems and the benefits which could result if the uncertainty were removed, we examine several potential applications for explosive driven MHD generators.

To summarize the findings of this report we conclude that not much has happened in the past decade. There have been experiments (12) which showed an increase in the chemical to electrical conversion efficiency, an experiment using a superconducting magnet (13), and a small number of theoretical or analytical papers (1-19). After all of this time the two basic questions remain:

1. What is the high-density plasma conductivity mechanism, and,
2. How long can pulses from an explosive driven MHD generator last?

In Section 3 of this report we conclude that circulating currents in the plasma coupled with a thermal ionization instability (14) in the plasma are probably responsible for the conductivity observed in the generator. It is also speculated that the conductivity in the high-pressure, low temperature, plasma may be described as due to overlapping wave functions (15). However, the more practical problem of maximum pulse duration remains unresolved. The circulating current models suggest that much longer pulse lengths can be achieved, but experimental verification is needed.

2.0 REVIEW OF EXPLOSIVE DRIVEN MHD POWER GENERATION

The first studies of explosive driven MHD generators (1), were sponsored by the Defense Advanced Research Projects Agency (ARPA) in 1962. These studies, which continued with an Air Force sponsorship until 1966, were based on about 700 tests or shots in four different sizes of generators (2-7). In these tests a wide variety of resistive and reactive electrical loads were used and a number of physical and electrical parameters were investigated. Before proceeding on this discussion, it appears appropriate to describe the explosive driven MHD generator and review some of the findings from these previous studies.

2.1 EXPLOSIVE DRIVEN MHD GENERATOR DESCRIPTION

The basic components of an explosive driven MHD generator are shown in Figure 2.1. A seeded explosive charge is placed at the entrance to the MHD channel. Detonation of the charge produces a moving "slug" of plasma which travels down the channel with an effective velocity, u . The channel has a transverse magnetic field, B_0 . The channel has a width, b , and an electrical separation or height, d . Electrodes in contact with the moving plasma, of length l_e , allow currents to be driven through an external load which has a load resistance, R_e , and an external inductance, L_e . In addition to interacting with the magnetic field, the rapidly expanding detonation products interact with the gases initially present in the channel inducing shock heating and pushing them down the channel. As of 1967, a rather clear physical picture of what goes on in an explosive driven MHD channel began to emerge.

The key observation was that the "armature" of the explosive driven MHD generator is a highly conductive plasma moving at about 8 Km/sec down the channel. The conducting zone, a , is a few centimeters thick near the explosive charge, growing to about 0.2 m thick about a meter from the charge. Near the explosive charge, a conductivity, σ , of about 1100 mho/m was measured (1).

2.2 ELECTRICAL PARAMETERS

The following sections summarize the observations relating to changes in electrical parameters.

2.2.1 Initial Magnetic Induction, B_0

It was shown that for nine separate magnetic inductions, from 1.2 to 2.6 Tesla, in three different sized generators, the peak power output scales as the square of the magnetic induction, B_0^2 .

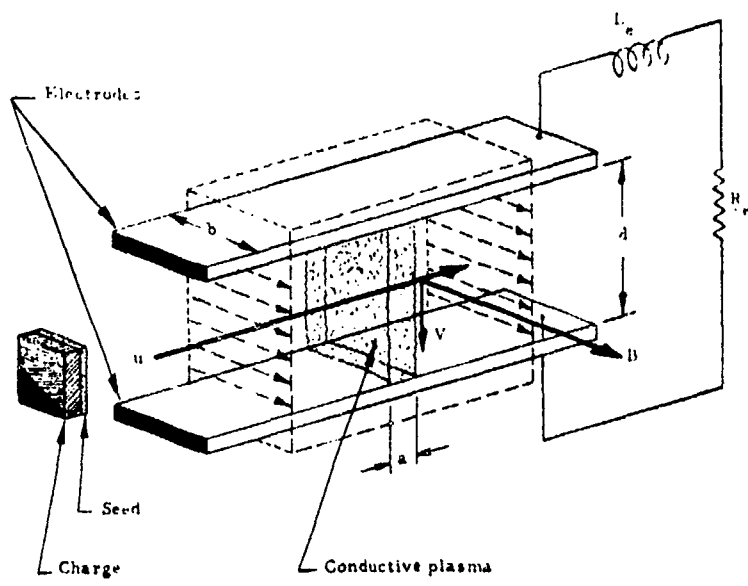


Figure 2.1
GENERALIZED MHD GENERATOR CIRCUIT

2.2.2 Pulse Length

From six different sets of experiments with electrode lengths, l_e , 0.02 m to about 1 m, it was shown that pulse length varies approximately as the electrode length.

2.2.3 Generator Size

Using data from three different sized linear generators, it was shown that the peak power varies directly with the generator cross-sectional area if the magnetic induction, plasma velocity, and seed level are equal.

2.2.4 Generator Load

It was demonstrated that there is an optimum load for a generator, and that the placement of the load was important. Peak power was achieved when the external load, R_e , matched the apparent generator internal resistance, R_i . These two observations correlated with a model where the internal resistance of the generator, R_i , can be described as about 40 milliohms per square of channel cross-sectional area (which implies a constant ca product), and a model where motion of the plasma slug either increases or decreases the inductance of the generator. If the generator is connected in a manner such that the magnetic field from currents in the electrodes adds to the static magnetic induction, B_0 , the effect is equivalent to adding a negative resistance term of magnitude, $\mu_0 B_0^2$, to the equation describing the generator behavior. These equations are discussed in more detail later in the report.

2.3 GASDYNAMIC PARAMETERS

These early tests clearly disclosed that the initial gas pressure in the channel should be as low as practical, without causing electrical breakdown between the electrodes and surrounding structures. Tests using nine different gases at pressures from less than 0.1 Torr to atmospheric pressure, showed that the peak electrical power output was essentially independent of initial gas composition, but depended primarily on initial density. Tests using helium, neon, argon, and krypton showed slightly longer pulse lengths, which implied that shock-heated gases were playing some role in the armature conduction mechanism, but did not markedly change the peak power output. A review of some of this data is presented in Section 3.1.1.

Electronegative gases, such as SF_6 or air, frequently gave better results because they prevented electrical breakdown of electrodes to the channel

end-flanges. It was quite clear that the primary conduction path for the current was through the plasma slug and that operation of the generator was almost independent of the chemical or ionization properties of the gases initially in the channel. The major role played by these gases is that they represent a mass which must be accelerated by the detonation products as they sweep down the channel.

2.4 EXPLOSIVE PARAMETERS

Five different explosive compositions were used; PETN, RDX, HMX, PBX, and Composition C-4, which is RDX with a mineral oil binder. The results appeared to be independent of chemical composition, i.e., oxygen balance; and depended upon physical parameters such as detonation velocity and energy release. The explosive loading density investigated went from 2 to 16 Kg/m² of channel area in seven steps. The optimum range appeared to be 12 Kg/m², i.e., further increases in loading density did not increase the peak power output from generators of the lengths covered in these studies.

2.5 SEEDING PARAMETERS

Three separate seeding elements were investigated; cesium, potassium, and sodium, as picrates, nitrates, and chlorides. The chemical form of the seeding compound was usually unimportant. Both surface seeding and bulk seedings were investigated. The conclusions were that seed placement was important, i.e., surface seeding was apparently superior to bulk seeding. Additional data on the subject of surface seeding versus bulk seeding is given in Section 3.1.2 of this report. In most experiments, cesium salts and potassium salts gave almost identical results. An optimum surface seed level was identified. Further increases in seed levels did not increase the apparent conductivity, but slowed down the expansion of the detonation products, thus reducing the peak current generated.

2.6 MAJOR PROBLEM AREAS

At the conclusion of the above referenced studies, there appeared to be a clearly defined set of parameters which could be used to design explosive driven MHD generators to produce high-power pulses over a broad spectrum of pulse lengths. The major uncertainties at that time were:

1. What is the basic conduction mechanism in the seeded detonation products?

2. What is the reason for the apparent high internal inductance of the MHD plasma slug?

3. What is the maximum length pulse which can be produced in an explosive driven MHD generator?

The objectives of our present study were to examine the first two questions. Our approach has been to critically review previously published analytical and experimental work on explosive driven MHD generators, and to conceptually investigate various mechanisms which could lead to the observed physical results. The question of a maximum pulse length for explosive driven MHD generators can only be answered by experiment. As we will see in Section 4, many applications require pulse lengths half an order of magnitude longer than pulses that have previously been demonstrated. Having arrived at a position where we dimly understand what goes on in short generators, more experimental data is needed to extrapolate these concepts out in time and space, as the detonation products expand. Determination of long duration pulse experimental data should be one of the next major goals in the study of explosive driven MHD generators.

3.0 ANALYTICAL STUDIES ON EXPLOSIVE DRIVEN MHD GENERATORS

3.1 REVIEW OF PREVIOUS DATA

Several recent authors have examined explosive driven MHD generators (8,11). In analyzing their work, which is reviewed in Appendix A, it became apparent that certain fundamental facts were being overlooked. It, therefore, appears appropriate to re-interpret some of the earlier data and present clear-cut examples of the questioned physical phenomenon from unpublished data.

3.1.1 The Role of Shock-Heating in the Explosive Driven MHD Generator

One of the frequently addressed assumptions is that the conductivity is caused by shock-heating of gases originally in the channel and that proper manipulations of the shock relationships will yield answers relating to the expected behavior of the explosive driven MHD channel.

As discussed in Section 2, the body of experimental evidence is that the MHD interaction is primarily with the seeded detonation products. Table III-1 presents data on a series of tests in the 4" x 1" channel, using two surface seeded 60° cone charges, where the gas type and initial pressure were varied in a systematic fashion to demonstrate the relationships between the MHD interactions and the shock-heating of the gases originally in the channel. The magnetic induction was 2.3 Tesla and the initial pressure ranged from 1 Torr to 200 Torr for this series of shots. While the data in this series only goes down to 1 Torr, another series of tests, run at lower pressures, down to 30 microns, showed that the channel behavior below 1 Torr initial pressure was essentially independent of pressure, providing electrical breakdown did not occur. These tests are discussed in detail in (4). Unfortunately, the data notebooks for those tests are not available and further analysis is not possible.

The peak current achieved in these shots using load resistors of 6.9, 18, and 35 milliohms, is shown in Figure 3.1 for helium and argon gases as a function of the initial pressure. It is seen that the highest current, and hence, the highest power outputs, were achieved at the lowest pressures.

Some understanding can be gained by examining the change of pulse length as a function of initial pressure.

TABLE III-1 DATA FROM TESTS IN 1" x 4" EXPLOSIVE DRIVEN
MHD GENERATOR USING HELIUM AND ARGON AT
VARIOUS PRESSURES AS THE INITIAL FILLING
GAS. B = 2.3 Tesla, 2-60° CONE CHARGES,
200 mg Cs PICRATE SURFACE SEED.

Ref. No.	Gas	Pressure (Torr)	R _L (Ohms)	I _{max} (kA)	V _{max} (Volts)	T _{peak} (μsec)	T _f (μsec)
15	He	10	0.035	17.0	900	23	-
16	He	30	0.0069	46.0	380	53	45
17	He	100	0.0069	30.0	220	54	44
18	He	30	0.025	17.1	800	33	40
19	He	100	0.024	20.9	630	33	42
20	He	30	0.024	18.2	620	36	44
21	He	10	0.024	22.5	720	24	40
22	He	30	0.024	23.6	810	27	40
23	He	100	0.024	23.0	700	29	40
25	Ar	10	0.0069	39.6	290	40	56
26	Ar	30	0.0069	38.6	295	46	59
27	Ar	60	0.0069	36.4	275	49	66
28	Ar	100	0.0069	25.7	205	46	68
29	Ar	200	0.0069	18.2	140	39	74
30	Ar	10	0.018	25.0	600	37	50
31	Ar	30	0.018	22.5	540	38	52
32	Ar	60	0.018	20.0	480	38	56
33	Ar	100	0.018	18.2	385	32	60
34	Ar	200	0.018	13.9	280	38	70
36	Ar	10	0.035	16.6	720	21	48
68	Ar	10	0.035	18.2	860	21	30
37	Ar	30	0.035	15.5	600	20	51
38	Ar	60	0.035	14.5	720	21	50
39	Ar	100	0.035	12.8	650	24	63
40	Ar	200	0.035	11.2	450	27	75
62	He	10	0.0069	49.2	380	45	43
82	Ar	1	0.0069	47.0	380	36	42
83	Ar	1	0.018	30.2	740	22	43
63	He	10	0.018	28.9	720	27	44
64	He	10	0.018	28.9	710	26	41
66	He	10	0.035	19.3	960	18	41

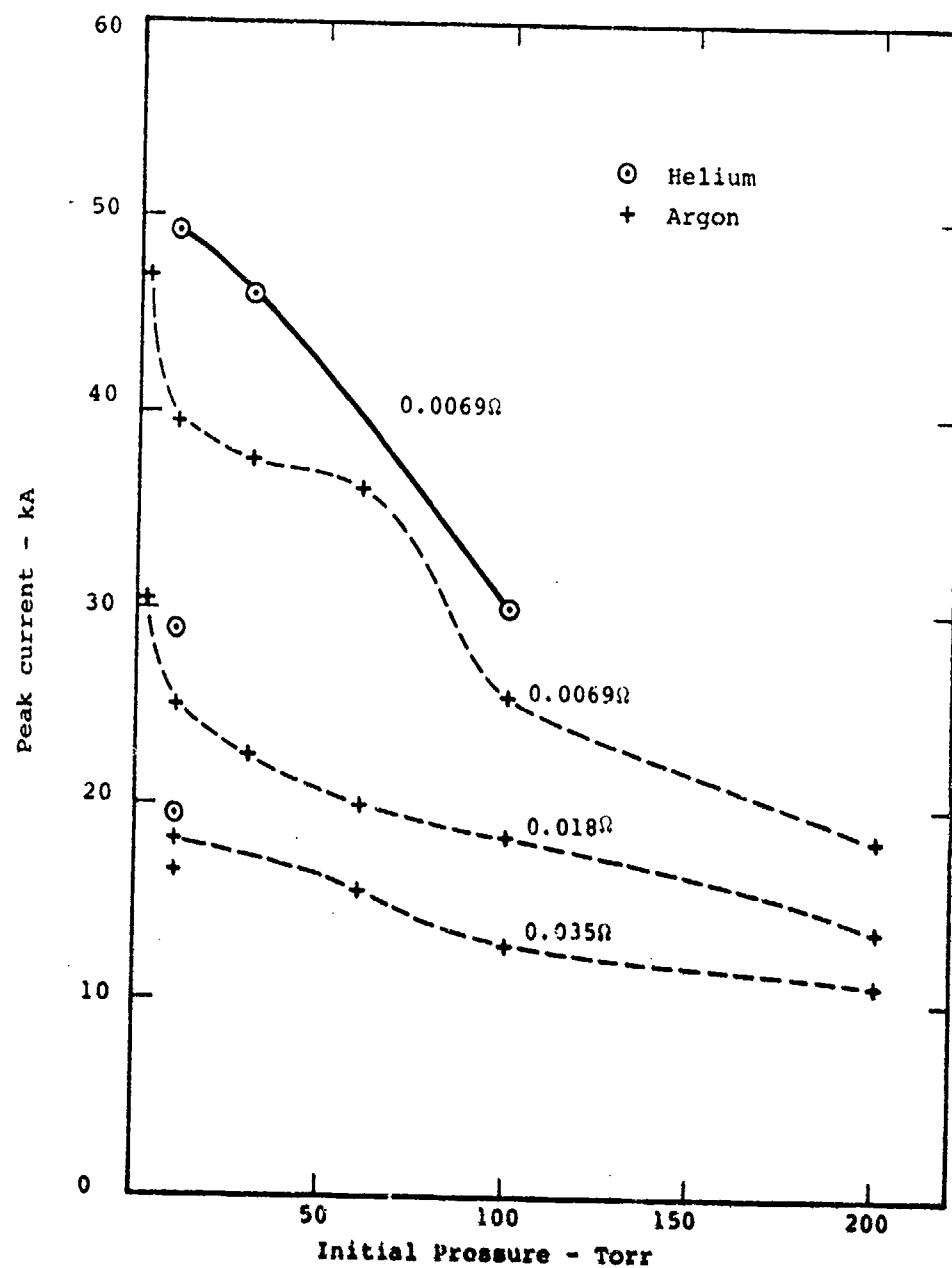


Figure 3.1

PEAK CURRENT IN EXPLOSIVE DRIVEN MHD GENERATOR AS A FUNCTION
OF PRESSURE OF HELIUM OR ARGON ORIGINALLY IN CHANNEL
FOR VARIOUS LOAD RESISTANCES

Figure 3.2 shows the time of peak current, and the time at which the current starts to fall rapidly (presumably when the conductive region leaves the ends of the electrodes), plotted as a function of initial pressure of helium or argon in the generator with a 6.9 milliohm load. It is seen for this low-load resistance that a low pressure of argon, 1 Torr, results in the current reaching its peak earlier and starting to fall earlier. This indicates, indeed, that there is shock heating of the argon which produces a conducting region. However, the peak current, due to both the seeded detonation products and the shock-heated argon, is not greater than that due to the seeded detonation products alone. As the initial argon pressure is increased, the peak current is reduced and the time scale of the pulse becomes longer.

The lengthening of the pulse and reduction in peak current at the higher pressures is compatible with a model where the residual gases slow down the plasma slug by increasing its mass. However, in the intermediate region, there is a suggestion that currents in the shocked argon allow joule heating which increases the conductivity. This can be seen in Figure 3.3, which is a V-I plot showing the peak currents plotted along each resistance line for the various initial pressures of helium and argon. It can be seen that for the shots with 100 and 200 Torr of argon initially in the channel, the net effect is to decrease the apparent open-circuit voltage from 1100 V to about 800 V and to increase the apparent generator internal resistance from 12 milliohms to about 23 milliohms for the 100 Torr case and to 38 milliohms for the 200 Torr case. This increase could come about through cooling and through a reduction in the time rate of change in inductance term ($dL/dt = \mu_0 \sigma u d/b$).

At the intermediate pressures, 10 Torr to 60 Torr, there is the suggestion that when the load resistance is reduced, and thus, increasing the current through the generator, the current heats the gas causing a change in the apparent internal resistance. At the lower pressures, 1 Torr, helium and argon give essentially the same results.

Unfortunately, only a few shots were taken at 1 Torr. However, it can be seen that the helium and argon data coverage at the lower pressures. The important observation is that for the load range of power production interest, i.e., the 20 to 30 milliohm loads (see Figure 3.1), the shock-heating is apparently not important, and the role of the gas as an insulator to prevent electrical breakdown becomes more important in producing a successful power pulse than its contribution to electrical conduction.

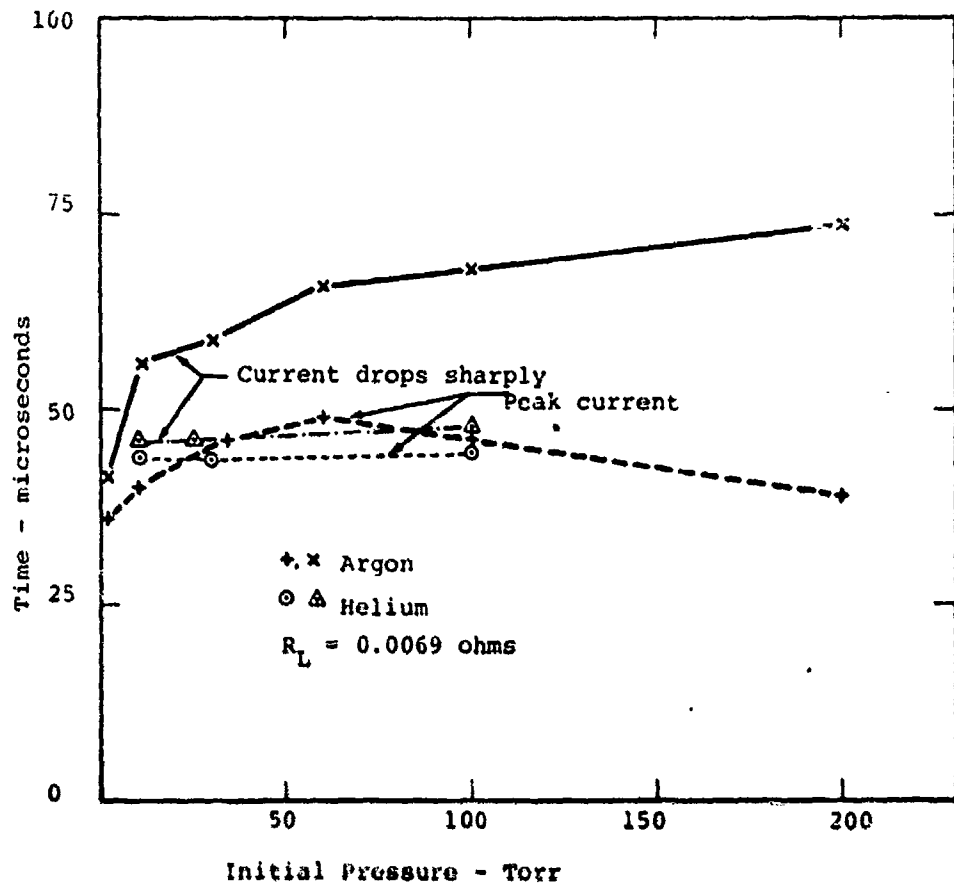


Figure 3.2
 TIME OF PEAK CURRENT AND TIME CURRENT
 STARTS TO DROP SHARPLY AS A FUNCTION
 OF INITIAL PRESSURE OF ARGON OR
 HELIUM IN CHANNEL OF EXPLOSIVE
 DRIVEN MHD GENERATOR

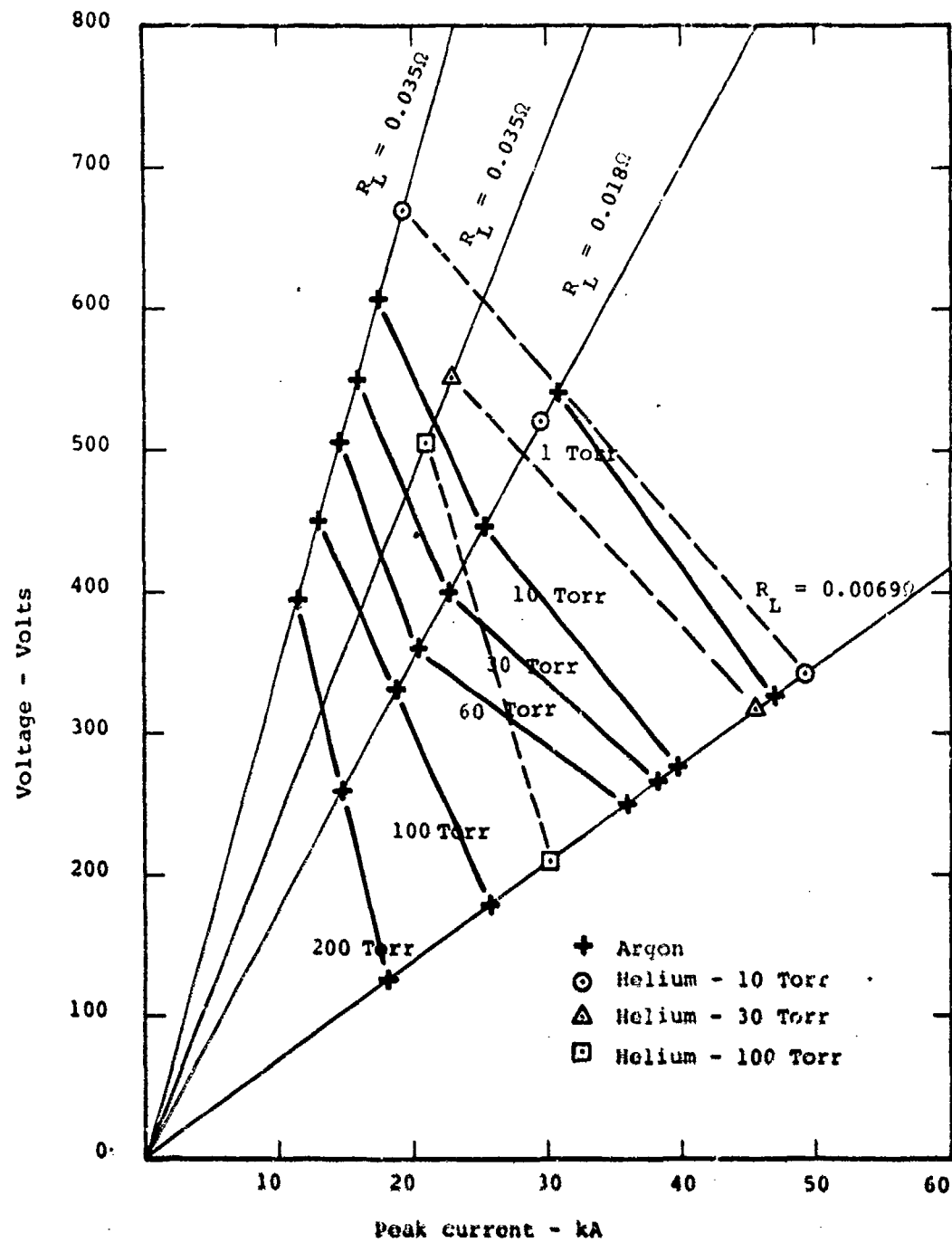


Figure 3.3

VARIATION OF PEAK CURRENT AS A FUNCTION OF
INITIAL PRESSURE OF ARGON OR HELIUM IN THE CHANNEL
FOR VARIOUS RESISTIVE LOADS

We conclude that although shock-heating effects can be observed in the operating regimes of interest, the primary conduction path in the explosive driven MHD generator is through the seeded detonation products.

3.1.2 Bulk Seeded Explosives

The question as to the best place to put the seeding in an explosive driven MHD generator appears to be unclear to some investigators. The original studies (1), compared 24% bulk seeded PBX (Plastic Bonded Explosive) charges with surface seeded RDX charges in the 1" x 1" generator and concluded that the bulk seeded charges might be superior. However, because of the difference in the mass of explosive in the two charges, .e., the PBX was heavier, the results were uncertain and could have been just due to the fact that more explosive was used. It was also shown that the combination of bulk seeding and surface seeding were the least desirable for those cases investigated.

Data is available for tests of bulk seeded charges which were performed under more carefully controlled conditions than those original tests.

The tests were made with PBX charges fabricated with 6, 12, 18, and 24% cesium nitrate. Two methods were used in evaluating the charges: (a) their effectiveness in producing pulses of power when driving an MHD channel, and (b) the peak current and current decay rate when driving a short-circuited generator. In the latter tests, controlled levels of surface seed were used on the various bulk seeded charges so that a surface seed equivalence could be used in evaluating the bulk seeding. These data are shown in Table III-2.

Figure 3.4 shows the performance of the 1" x 4" generator using single charges with a magnetic induction of 1.3 Tesla and 2 Torr of air in the channel. It is clear that the specially made bulk seeded PBX charges do not have the reproducibility that is observed with the commercially available RDX charges. This is particularly noticeable in the short-circuit shots where the variations in the peak current for the RDX shots is about 10% (which is larger than the normal variation of a few percent), while the bulk seeded charge current variation may be 50%. It is seen that for all load resistances used, the RDX charge surface seeded with 200 mg of cesium picrate produced a higher peak current than the bulk seeded charges. There is a suggestion from this data that the 18% seeding produces slightly more conductive detonation products than the other bulk seeded charges.

TABLE III-2 CURRENT DECAY TIME CONSTANTS FOR BULK SEEDED CHARGES
 IN 1" X 4" EXPLOSIVE DRIVEN MHD GENERATOR
 $R_L = 0.00025$ OHMS

Charge	Surface	Peak	Decay
	Seed	Current	Time Constant
	Mg Cs Picrate	kA	μsec
6% PBX	0	13.0	18.5
12% PBX	0	11.6	10.0
18% PBX	0	14.9	15.4
24% PBX	0	13.9	24.0
RDX	25	14.9	18.2
RDX	200	19.5	38.0
6%	200	19.1	35.0
12%	200	21.4	32.5
18%	200	17.6	25.5
24%	200	18.6	28.0
RDX	700	26.0	58.0
12%	700	22.3	47.0
18%	700	20.9	40.0
24%	700	20.0	43.5

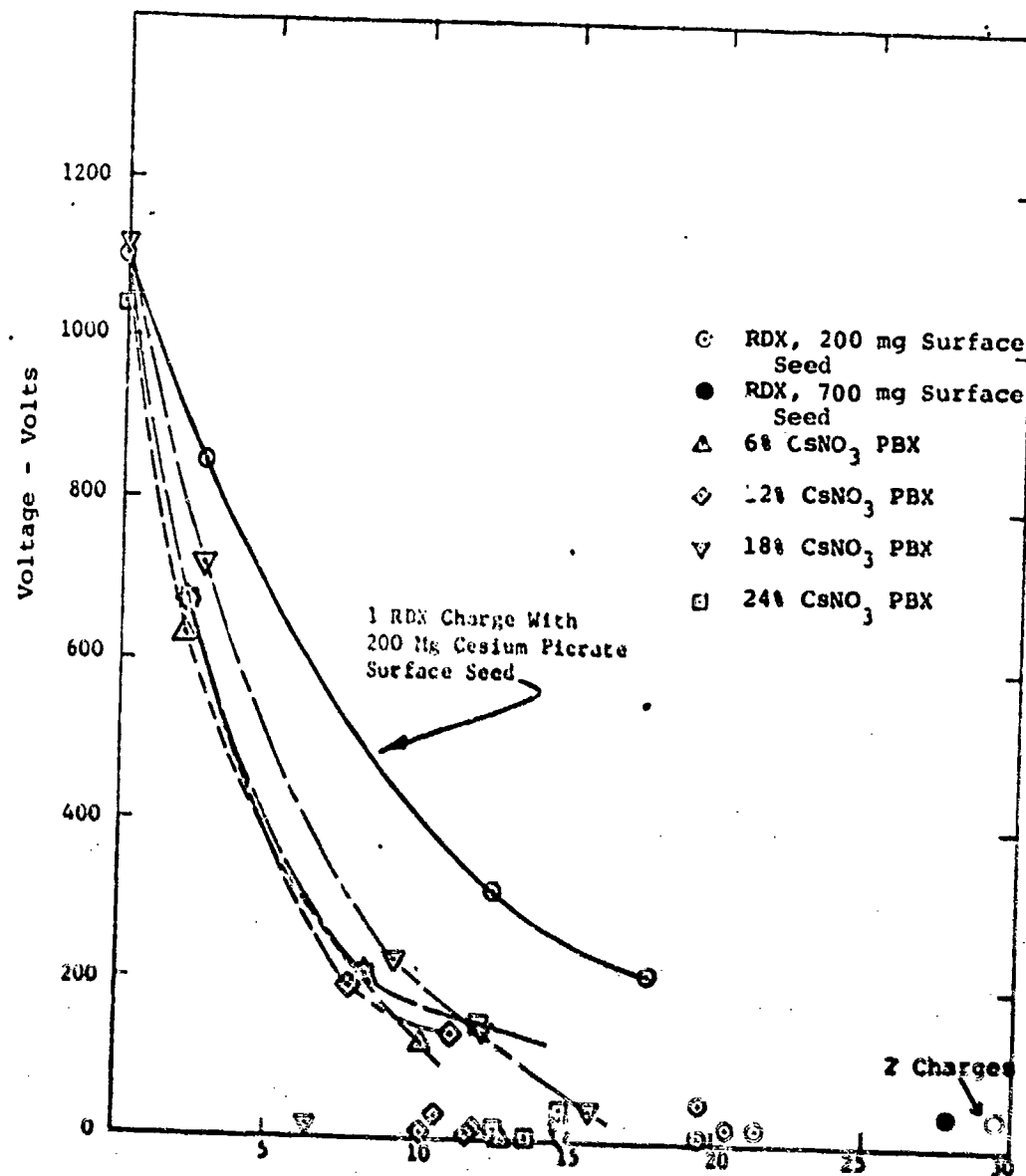


Figure 1.4

VOLTAGE CURRENT CURVES FOR BULK SEED PBX CHARGES.
ALSO SHOWN IS DATA FOR RDX CHARGE SURFACE SEEDED
WITH 200 MG CESIUM PICRATE.

One area of unusual behavior was noted in the low-load resistance regime where lowering the resistance did not result in a further increase in current. This results in sort of a "bending back" of the V-I curves shown in Figure 3.3. However, if the amount of seed used is increased, either by using two surface seeded charges, or increasing the seed used on one charge, the short circuit current increases. The oscilloscope traces for these shots show that the basic change in the pulse as the seed level is increased is to increase di/dt throughout the rising part of the current. Since everything else has remained constant, the major conclusion that can be drawn is that the seed level controls the generator internal inductance much more than it controls its internal resistance. This fact had previously escaped notice because all internal inductance measuring tests had been performed with standard seeding conditions.

Further insight on the relationships between surface seeding and bulk seeding can be gained by examining what happens when surface seeding is added to bulk seeding charges in a short circuit generator experiment. Here we have two somewhat independent measures of the plasma conductivity, the peak current and the rate at which the plasma current dies away, which is expressed in terms of the e-folding time constant, τ . While there may be some mechanism limiting the current build-up rate, the current decay rate should be relatively free from these influences and be more representative of the conductivity. Figure 3.5 shows the peak current achieved as a function of the amount of surface seeding used.

It can be seen that the peak current produced by the bare bulk seeded charges was less than the peak current produced by the RDX charges surface seeded with 25 mg of cesium picrate. It is also seen that when cesium picrate in small amounts was surface seeded on the 10t bulk seeded charge, the peak currents were higher than the same amount of surface seeding on the plain RDX charges. At the 200 mg level, the 10t bulk seeded charge and the surface seeded plain charge were again equivalent. At higher surface seeding levels, the surface seeded "plain" charges were superior to the bulk seeded charges.

The reason for this apparent adverse reaction between surface seeding and bulk seeding is not known and represents an important area for future investigation. Equally puzzling is the reason why the 10t bulk seeded charges appear to be superior to the other bulk seed levels investigated. One

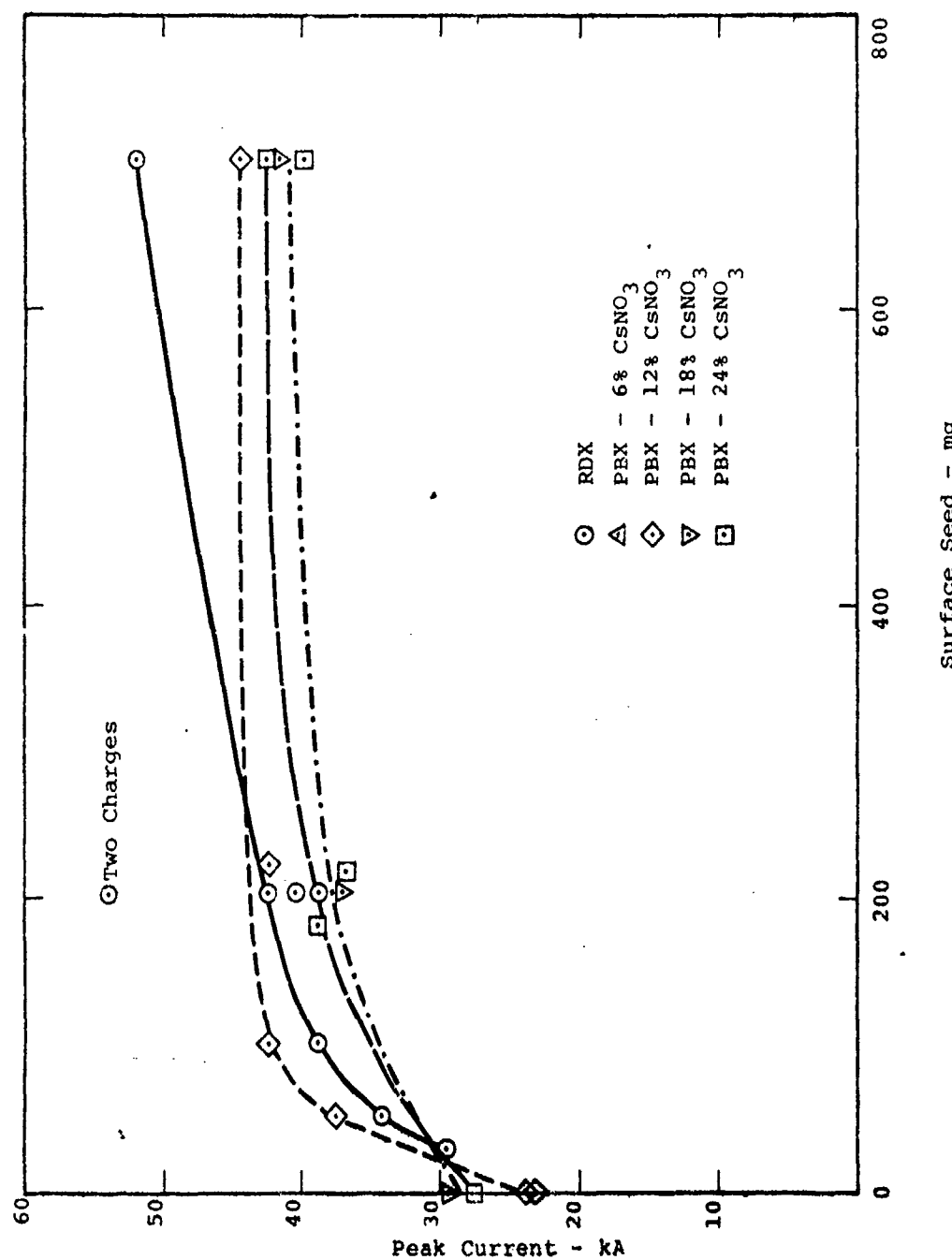


Figure 3.5

PEAK CURRENT IN EXPLOSIVE DRIVEN MHD GENERATOR
AS A FUNCTION OF MASS OF Cs PICRATE SURFACE SEED
USED WITH BULK SEEDED PBX CHARGES AND UNSEEDED RDX CHARGES

tentative suggestion is that the manufacturer mislabeled the charges and that the 18% charges were really the 24% bulk seeded charges. Unfortunately, the residual charge inventory was destroyed and chemical examination to support this conclusion is not possible.

The current decay time constants from these experiments are shown in Figure 3.6. In principle, the current decay time in an inductive-resistive circuit will be proportional to the plasma conductivity. The effect of seed level on current decay rates was examined in detail in (4). It is seen that for the surface seeded charges the decay time constant increases with seed level, indicating an increase in plasma conductivity.

We see for the bulk seeded charges that surface seeding increases the decay time constant, but in all cases with surface seeding greater than about 100 mg per charge the decay time constant for the bulk seeded charges is less than that which would have been obtained if the same amount of surface seeding had been used on an unseeded charge. Variation of the decay time constant for the bulk seeded charges in the range between 200 mg and 700 mg is another reason for suspicion that the 18% and 24% charge composition labels had been reversed. In the range below 100 mg of surface seed, the data is more difficult to interpret. One clear-cut conclusion that can be drawn is that surface seeding in excess of 100 mg per charge was superior to any bulk seeding investigated.

We conclude that for most applications, surface seeding of the explosive charge should be superior to bulk seeding. There is apparently a complex reaction between the surface seeding materials and the bulk seeded charges. Possible reasons for this interaction may be in the chemistry of the explosives, i.e., in this case RDX was used for the unseeded charges and PBX was the base for seeded charges. Further experimental work is very definitely needed to sort out and confirm the various effects before further analytical work can be initiated to explain these differences.

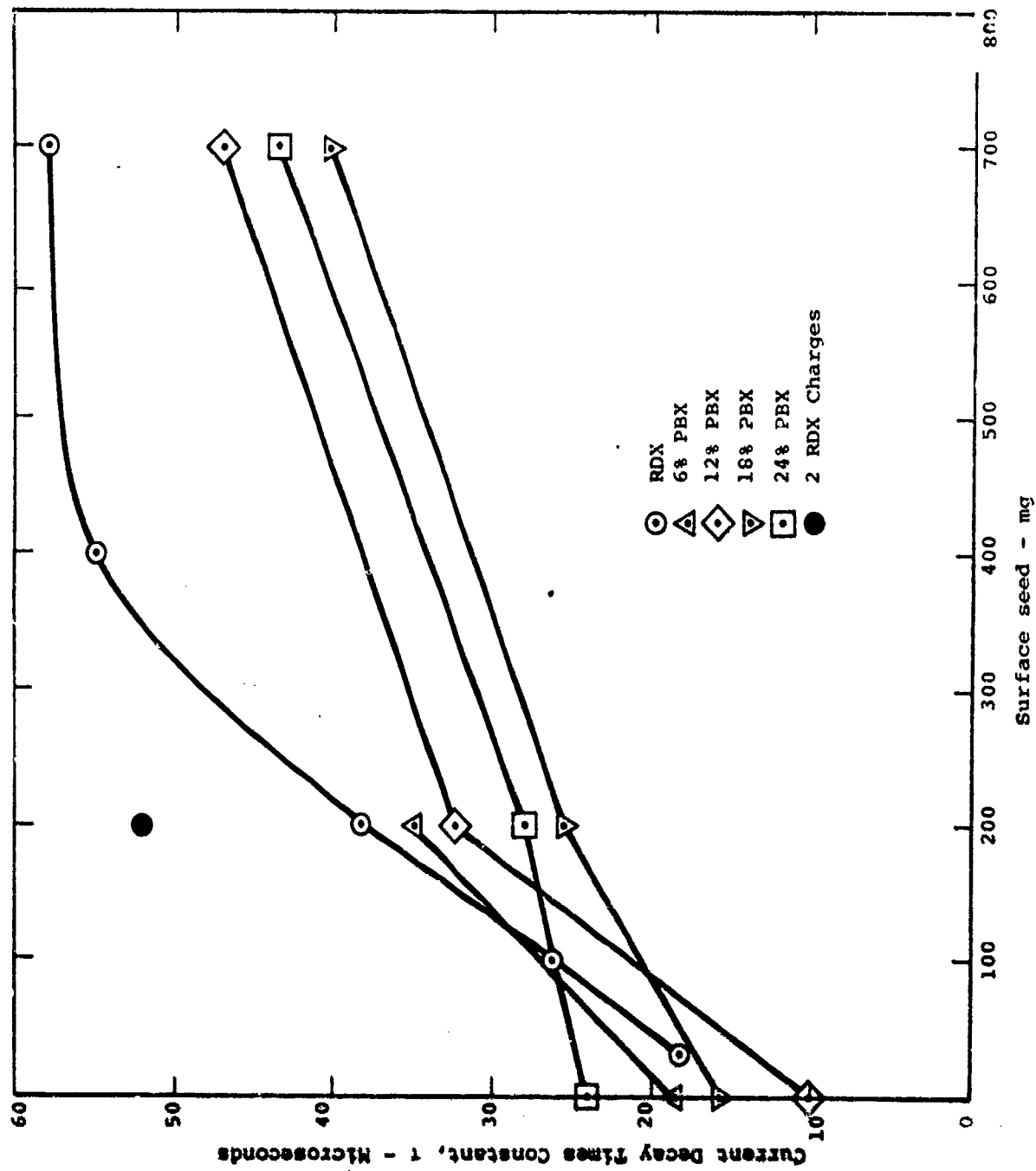


Figure 3.6

VARIATION IN SHORT-CIRCUITED GENERATOR CURRENT DECAY TIME, t ,
FOR BULK SEEDED PBX CHARGES AND UNSEEDED RDX CHARGES AS A FUNCTION
OF MASS OF CESIUM PICRATE SURFACE SEED USED.

3.2 CIRCUIT ANALYSIS

There have been a number of analytical studies of explosive driven MHD generators (8, 9, 11, 13). In a number of these, the analysis is presented in terms of the "magnetic Reynolds number", (R_m), which is defined by the non-dimensional set of parameters as

$$R_m = \mu_0 u \sigma x \quad (1)$$

where μ_0 = permeability of free space, u , is the velocity, σ , the conductivity, and x is a representative dimension in the direction of the velocity, u . As we shall see below, this dimensionless number occurs naturally in the description of the diffusion of magnetic flux into a moving conductor. However, care must be used when the magnetic Reynolds number concept is applied to the explosive driven MHD generator. For example, the condition $R_m = 1$, can be interpreted in terms of the magnetic fields induced in the plasma being of the same order of the applied magnetic field, B_0 ; however, this can only happen if there is some path for the induced current. The analysis must therefore account for the electrical field caused by the output current flowing through the external load when determining the magnitude of the induced magnetic fields. This means that it is not the plasma conductivity, σ , but a combination of the plasma conductivity and the electrical field, E , due to the external load which determines the current flow in the plasma.

In a generalized expression, we must use an external impedance, X_e , to determine the electric field due to the load, and hence, its time varying influence on the currents and magnetic field in the plasma slug. The message is that indiscriminate use of R_m in parametric studies may tend to obscure what is actually going on in the explosive driven MHD channel.

One of the interesting problems in explosive driven MHD generator theory is how to handle the induced magnetic fields. In the low magnetic Reynolds number approximation, the plasma is viewed as a long flat conductor of width b , and thickness a , carrying a current, I . The normal assumption is that the current density, j , will be uniform and is given as

$$j = \frac{I}{ab} \quad (2)$$

Neglecting end-effects (a one dimensional approximation), the induced magnetic field, B_1 , is found from Maxwell's equation,

$$\frac{\partial B}{\partial x} = -\mu_0 j \quad (3)$$

Under the assumption that the current density, j , is constant, we can integrate and apply the appropriate boundary conditions to arrive at a solution which has $B_i = 0$ at the center of the plasma, with induced magnetic fields which increase the magnitude

$$B_i = \pm \frac{\mu_0 I}{2b} \quad (4)$$

on the surface of the conductor. The net change in B , i.e., ΔB , when passing through the plasma is twice this value.

While nothing we have done this far is unusual, we note that in the plasma slug of an explosive driven MHD generator, the current density, j , is probably not uniform. There are two basic reasons for the non-uniformity: (a) the plasma may have a non-uniform velocity distribution, and (b), with high interaction parameters, the magnetic fields produced by the induced currents can cancel out the applied magnetic field in the interior of the slug. Both of these effects will be examined.

Because the front and back of the plasma slug move at different velocities, a circulating current must be set-up within the plasma slug when it is in a magnetic field. The same sort of circulating current can be set-up if the plasma slug is originally outside of the magnetic field region, and then passed through a field gradient into the constant field region. These two effects, either the velocity gradient or the magnetic field gradient, induce unequal voltages at the front and back of the slug. Circulating currents flow from the plasma to the conductive metallic electrode boundary, then back into the plasma at the other end, creating a current distribution which forces the plasma potential to match the equipotential established by the conductive boundary surface. With the plasma slug in the channel, the peak circulating current density at the plasma surface, j_i , produced by a velocity differential, ΔV , is given by

$$j_i = \frac{e \Delta V}{2} B \approx 10^3 \cdot \frac{2 \times 10^3}{2} = 2 \times 10^6 \text{ A/m}^2 \quad (5)$$

Correspondingly, a slug 0.02 m long traveling through a region with a magnetic field gradient of 20 Tesla/m, would have a circulating current density at the surface of.

$$j_1 = \sigma u \frac{\Delta B}{2} = 10^3 \cdot 8 \times 10^3 \cdot \frac{0.4}{2} = 1.6 \times 10^6 \text{ A/m}^2 \quad (6)$$

which is the same order of magnitude as the current density due to velocity differential.

Assuming that the current density, j_1 , is not large enough to cause joule heating which would result in a non-uniform conductivity distribution, the circulating current density due to differential motion or magnetic gradients, would be linear from $+j_1$ at the front, falling through zero at the center of the slug, going to $-j_1$ at the rear. These two effects are independent, and hence, additive.

There is the possibility that these circulating currents acting on a low temperature (3000° K) low conductivity (100 mho/m), high pressure (300 atm) alkali metal plasma could produce a high conductivity (1000 mho/m) surface layer. Unfortunately, the indicated heating rates are about two orders of magnitude too low to explain the observed high conductivity.

One other potential mechanism to explain the high conductivity may be the "T-layer" observed in explosive driven shock tube experiments (14). The description of a T-layer is that if the electrical conductivity of the medium increases with an increase in temperature and a perturbation occurs which causes the electrical current, which is flowing through it while in a magnetic field, to increase the joule dissipation such that an increase in temperature occurs, then this perturbation will develop into a T-layer. This is in essence a thermal instability of the type which usually causes arcs to form, but in this case where there is a transverse magnetic field, it appears as a layer. The authors (14) describe the currents necessary to initiate the T-layer (17 kA) as only slightly greater than the eddy currents appearing in the region where the magnetic field is not uniform (-10 kA). Figure 3.7 which is reproduced from (14) shows the T-layer starting to grow from an initial current density of $3 \times 10^6 \text{ A/m}^2$. We conclude that a thermal instability mechanism similar to the T-layer undoubtedly plays a dominant role in some of the experiments, i.e., the intermediate pressure argon experiments described in Section 3.1.1 where the current voltage relationship goes non-linear. However, we must note that our original conductivity measurements, Figure 2.17 of (1), which were made without any magnetic field, gave conductivities of the order of 1000 mho/m . We must therefore conclude that while T-layer effects may contribute to the conduction

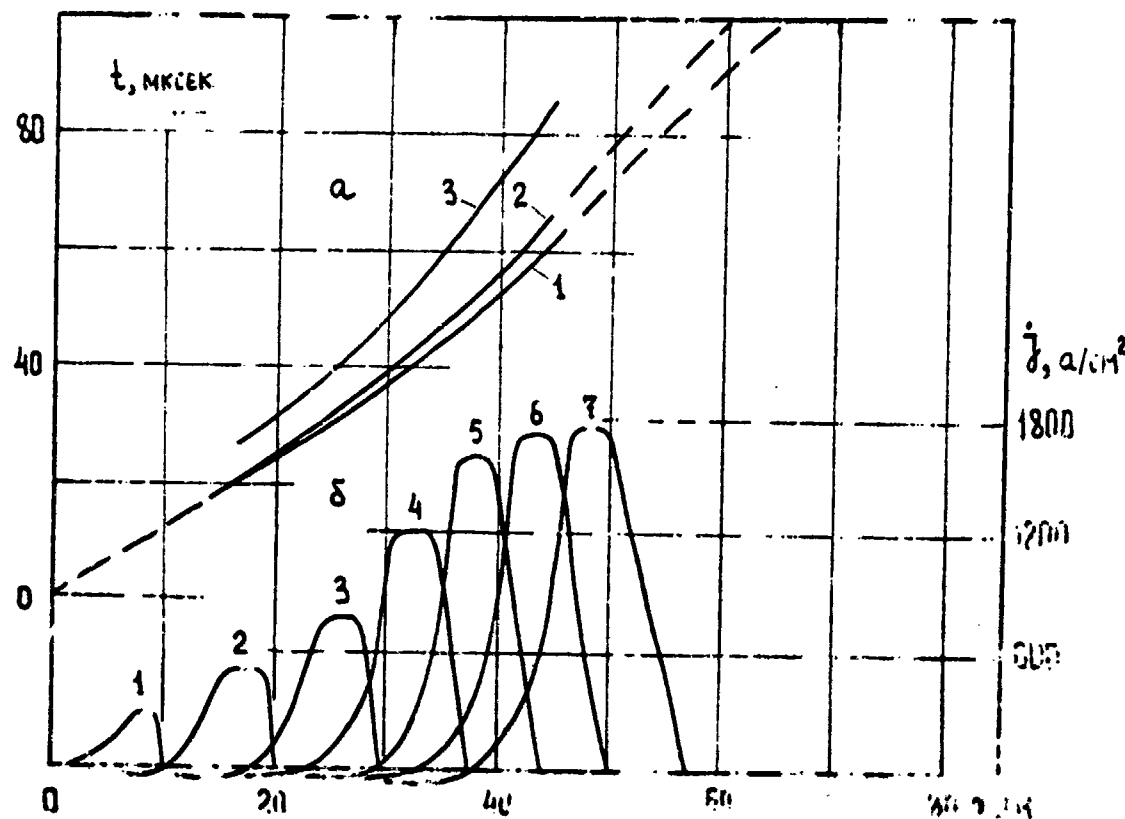


Figure 3.7

TIME-SPACE DIAGRAM FOR THE MOVEMENT OF PLASMA IN A MAGNETIC FIELD AND CURRENT DENSITY DISTRIBUTION;
 A-I-FRONT OF A REFRACTED WAVE;
 2-FRONT OF LUMINESCENCE;
 3-BOUNDARY OF THE NONELECTROCONDUCTIVE ZONE;
 B-1-12 MICROSECONDS FROM THE START OF THE CURRENT;
 2-24; 3-36; 4-48; 5-60; 6-72; 7-84.
 (After Asinovskii, et al (14))

mechanism responsible for the observed conductivity in seeded detonation products when in an MHD generator, they are not the mechanism which causes the initial conductivity.

A second effect which may be important is the tendency for the plasma slug to maintain a constant magnetic flux within its boundaries. Assuming that the slug is formed in a field-free region and then is rapidly passed into a region containing a magnetic field, the plasma appears diamagnetic in that a system of currents is induced in the edges of the slug to cancel out the flux in the interior trying to keep the net flux, ϕ , equal to zero. In this case, the application of Maxwell's equations and Ohm's law gives

$$\frac{\partial B}{\partial x} = -\mu_0 j = -\mu_0 u_0 B \quad (7)$$

With the plasma in contact with the electrodes we have the one dimensional solution

$$B = B_e \exp(-\mu_0 u_0 x) \quad (8)$$

Where B_e is the external magnetic field. This then requires that

$$j(x) = u_0 B_e \exp(-\mu_0 u_0 x) \quad (9)$$

The surface current density per unit width, j_s , is obtained from integrating with respect to x

$$j_s = u_0 B_e \left[\exp(-\mu_0 u_0 x) dx \right] = -\frac{B_e}{\mu_0} \quad (10)$$

This result is valid if the dimension of the slug, a , is such that the quantity $\exp(-\mu_0 u_0 a)$ is small. $B_e = B_0$ if no currents are flowing through the external load circuit.

The first comment we can make is that the current density along the edge of the plasma slug ($x = 0$) can be as high as

$$j(0) = u_0 B_0 \approx 10^3 \cdot 8 \times 10^3 \cdot 2 = 1.6 \times 10^7 \text{ A/m}^2 \quad (11)$$

As we have seen above (14), the T-layers are observed starting at current densities of about $3 \times 10^6 \text{ A/m}^2$. We can, therefore, postulate that with initial conductivities as low as 200 mho/m local joule heating due to the plasma diamagnetic effect can be sufficient to increase the conductivity to the observed values within the time scale of the experiment. The rate of heating depends linearly on ϵ , hence, as T increases, so does ϵ , therefore the rate will accelerate. Correspondingly, we might observe that the plasma diamagnetic effect

is one mechanism which could maintain high surface conductivities as the plasma expands while it moves down the channel. We may note that the current couple necessary to maintain the diamagnetic effect is

$$j_{dm} = \frac{B_0}{\mu_0} \approx 1.6 \times 10^6 \text{ A/m} \quad (12)$$

For our 1" x 4" channel measurements, this current couple would be ± 40 kA, which is of the order of magnitude of the observed load current. This analysis implies that most of the diamagnetic current is carried in a band at the front and rear of the slug, whose thickness, ξ , is given as

$$\xi \approx \frac{1}{\mu_0 \sigma u} \approx 10^{-1} \text{ m} \quad (13)$$

If we assume that this current couple is carried in a loop of dimensions a long by d high, and b deep, with the resistance produced by the two bands ξ thick, the current decay time is $1/2 \mu_0^{-1} \sigma^2 a u$ which is of the order of 1 msec for these conditions.

The current density in the plasma slug when the generator is under load is also of interest. If we neglect the gradient and diamagnetic effects and assume a uniform slug moving at a uniform velocity, we have

$$\frac{\partial B}{\partial x} - u_0 j = -\mu_0 \sigma (uB - E) \quad (14)$$

where $E = V/d$, is the field due to the load. Rearranging terms we get the equation

$$\frac{\partial B}{\partial x} + \mu_0 \sigma u B(x) = \mu_0 \sigma E \quad (15)$$

which has the solution

$$B = \frac{E}{u} (1 - \exp(-ux)) + B_1 \exp(-ux) \quad (16)$$

$$\text{where } B_1 = B_0 + B_L \quad (17)$$

and

$$u \approx \mu_0 \sigma u = \xi^{-1} \quad (18)$$

and B_L is the field at the surface of the plasma due to the load circuit. This is similar to the results derived by Sinkevich and Krylova (1). When $E = 0$, i.e., the short-circuit case, the field in the front of the slug is given as

$$B = B_0 \exp(-ux) \quad (19)$$

and the field at the rear of the slug, B_2 may or may not equal B_0 , depending

upon the total amount of flux available for the experiment and its distribution inside and outside of the generator (1-19).

In a load circuit where the electrodes are broad flat conductors which represent a single turn, and the channel width, b , is greater than the height, d , the load circuit magnetic field is given as

$$B_L = \mu_0 \frac{I}{b} \quad (20)$$

When the generator is connected such that the system inductance increases with time, the field at the rear of the slug, B_2 , is

$$B_2 = B_0 - B_L = B_0 - \mu_0 \frac{I}{b} \quad (21)$$

When considering circulating currents and the diamagnetic effect, we note that the current screening out the field at the rear of the slug is generated by the front, and that the current path appears to be in parallel with the external load. The field inside of the rear of the slug is given as

$$B = B_2 \exp(\alpha(a-x)) \quad (22)$$

We therefore have the situation where

$$\int j_+ dx = \frac{I}{b} + \int j_- dx \quad (23)$$

j_+ is the current density in the front of the slug, j_- the current density in the rear, and the current density is zero at the point, c . We know from (10) that for the full diamagnetic effect the second integral is B_2/μ_0 . The first integral is evaluated by substituting the appropriate value of B from equation (16), and noting that

$$E = \frac{IR_L}{d} \quad (24)$$

to obtain

$$(B_0 - \mu_0 \frac{I}{b} - \frac{IR_L}{ud}) (1 - e^{-\alpha x}) = \mu_0 \frac{I}{b} + B_2 \quad (25)$$

If $\alpha c > 1$, we then have

$$I = \frac{(B_0 - B_2)}{\frac{R_L}{ud} - \frac{2\mu_0}{b}} \quad \text{or} \quad \frac{(B_0 - B_2)}{\frac{R_L}{ud}} \quad (26)$$

We may further note that since the front and rear of the real plasma slug have different velocities, the magnetic diffusion length in the slug is a function of position, even if the conductivity is constant. Some authors would interpret this by saying the back and the front of the slug have different "magnetic Reynolds numbers".

This means that both u and B in equation (14) are functions of x . We describe the variation in velocity as

$$u = u_f(1-\beta x) \quad (27)$$

where the velocity ratio $u_s/u_f = \psi$, so that

$$\beta = \frac{(1-\psi)}{a} \quad (28)$$

where a is the plasma slug thickness. Substituting in (14) we have

$$\frac{dB}{dx} = -\mu_0 j = -\mu_0 \sigma (u_f(1-\beta x)B(x) - E) \quad (29)$$

which has the solution

$$B = \exp(\mu_0 \sigma u_f \frac{(x-\beta x^2)}{2}) \{ \mu_0 \sigma E / \exp(-\mu_0 \sigma u_f \frac{(x-\beta x^2)}{2}) dx + C \} \quad (30)$$

which can be evaluated in terms of $\text{erf}(ix)$.

We can see that the velocity gradient has the effect of increasing the diffusion of flux into the conducting slug, but not reducing the surface current density.

The current distributions which we have postulated should be measurable with careful magnetic probe or optical spectroscopy techniques. Details of the current structure of the nature of those shown in (14) provide valuable insight into the conduction mechanism. While these mechanisms may be responsible for the maintenance of the electrical conductivity, they do not appear to provide an adequate explanation for the conductivity observed in the absence of a magnetic field. To answer this aspect of the problem, we may note that theoretical work by Alexeev (15) and experimental work by Kulik (16) show high conductivities in high pressure (100 - 1000 atm) cesium plasmas in the temperature range of interest. An overlapping wave function mechanism described by Alexeev could be responsible for the conductivity of the needed detonation products in the region near the explosion.

We, therefore, conclude that while circulating currents and/or T-layers may enhance the conductivity of the seeded detonation products, they do not appear to be the mechanism which is responsible for causing the initial high-electrical conductivity observed in the seeded detonation products. The strong variation of σ with temperatures suggested by the Alexeev model suggests ways that measurements of conductivity in the regions very near the explosive charge could be used to test the applicable theories.

4.0 SCALE-UP OF EXPLOSIVE DRIVEN MHD GENERATORS

While the demonstrated power output with explosive driven MHD generators has been interesting, i.e., 230MW reported (5), and 129MW reported in (12) which is discussed in Appendix A, there has been a continuing interest in what large scale explosive driven MHD channels would look like and how they would perform. At this point, it appears appropriate to examine in detail a large scale (5MJ) explosive driven MHD generator which has previously been proposed (8), and to outline other potential designs of interest.

4.1 5MJ DESIGN STUDY

The goal of this study was the rapid, repetitious production of 5MJ pulses with a duration of 100 microseconds feeding a 1 ohm load.

The first characteristic examined was charge geometry. It has been evident from the first experiments in 1961, that the efficiency of the explosive driven MHD generator could be improved if the solid angle subtended by the generator at the charge surface could be increased. The logical solution for rapid repetitive pulsing was to use back-to-back channels facing a single explosive charge.

The second parameter to be examined was channel geometry. One of the principle functions of the channel is to act as a containment vessel for the detonation products. The most efficient shape for containing internal pressures is the cylinder. This dictates that the pressure vessel be cylindrical to reduce material stress levels. In order to have an efficient magnet system, it is important to have the channel fill as much of the containment vessel as is practical, inasmuch as the containment vessel defines the region where the magnetic field is available. This then implies that the channel should also be cylindrical.

Extensive experimentation has shown that the generator internal resistance is between 5 and 10 ohms per square in the configuration where the generator inductance decreases with time. Therefore, to produce a pulse which can directly and efficiently couple into a 1 ohm load would require an effective channel height to width ratio of 100 to 200 to 1. This can be achieved by subdividing the channel and connecting adjacent elements in series. Figure 4.1 shows a way that adjacent rectangular channels could be connected together through the subdivision partitions to effectively change the channel height to width ratio, and hence, the internal resistance. Because of the short pulse length, the current

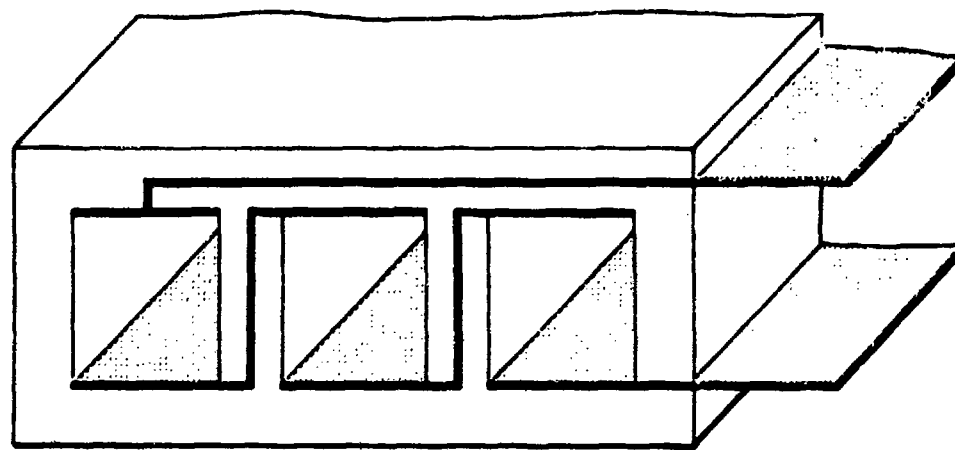


Figure 4.1

METHOD OF INTERCONNECTING EXPLOSIVE DRIVEN MHD CHANNELS TO INCREASE GENERATOR INTERNAL RESISTANCE

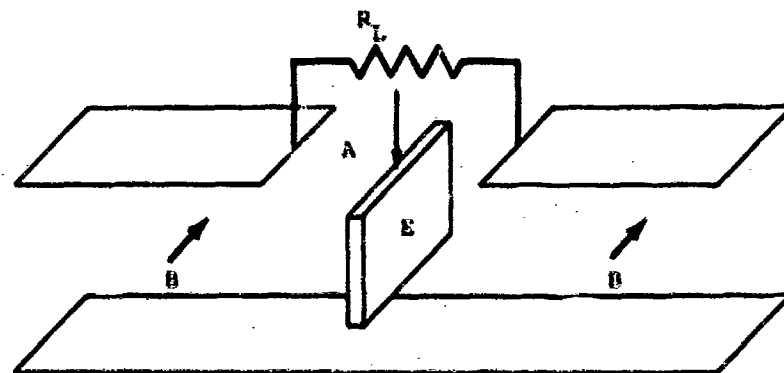


Figure 4.2

METHOD OF CONNECTING BACK-TO-BACK EXPLOSIVE DRIVEN MHD CHANNELS TO INCREASE GENERATOR IMPEDANCE.
EXPLOSIVE CHARGE E SHOULD BE INITIATED AT POINT A.

only flows in a thin layer on the surface of the conductor; therefore, thin foils mechanically supported by the plastic separator can be used as the electrodes and interconnecting strap.

Another effective way of increasing the generator internal resistance is to connect the generator to the load in a manner such that the inductance increases with time, rather than as a flux compression device. In this configuration, the generator internal resistance appears to be of the order of 50 milliohms per square, which would then only require a 20 to 1 channel aspect ratio. By putting the two channels on opposite sides of the charge in series, as shown in Figure 4.2, the effective aspect ratio for each generator need only be 10 to 1, which may be mechanically achievable.

As we have seen in Section 3.1.1, the explosive driven MHD generator efficiency is highest when the channel is evacuated to nearly 1 Torr. For repetitive pulsing at the rate of several per second, a giant vacuum pumping system would be required to evacuate about 50 m³ of detonation products after each shot. An analysis indicated that the system could be simplified and made more reliable if the seeded charge and the generator electrodes were sealed in an evacuated plastic assembly which could be slid into place in the cylindrical containment vessel. Design analysis disclosed that the containment vessel could also serve as the "warm" bore for a superconducting magnet. This approach eliminates the need for a vacuum pumping system.

The need for a superconducting magnet arises from the desire to make the explosive charge a reasonable thickness. The pulse duration determines the electrode length. Therefore, to obtain a desired stored magnetic energy,

$$E_{mag} = \frac{1}{2} \frac{B^2}{\mu_0} \cdot b^2 d v \quad (31)$$

within the generator volume, the $B^2 db$ product will be constant (where d is the channel height and b the width) since the length v is constant. One of the design parameters is that the output will be a prescribed fraction of E_{mag} . The choice of the magnetic induction B establishes the channel cross-sectional dimensions. The explosive loading is designed on the basis of so many kg per square meter of flow area, with the total energy release E_{expl} equal to the total charge weight times the energy release per unit mass. For a constant ratio of E_{expl} to E_{mag} , the charge becomes thinner as B is decreased. Thin charges are

harder to initiate uniformly and to support during rapid movement. The most practical way to initiate charges for this application appears to be through the median plane on the side away from the continuous electrode, as shown in Figure 4.2.

A conceptual design for such a generator, based on a 5 Tesla superconducting magnet, is shown in Figure 4.3. The magnet has a 1 m warm bore. With a 1 ohm load specified, the current and voltage are equal at 235 Kv and 235 KA, producing 5×10^{10} w. With a pulse length of 10^{-4} sec, the energy output is 5MJ. If the external load inductance is reasonably low, a 25 Kg charge should be able to produce this energy from a two-channel generator assembly with a total length of about 5 m.

The rate of firing is controlled by the mechanical limitations of placing a new channel in the magnet for each shot. With the lightweight replacement channels being constructed of plastics, pulse repetition rates of a few per second should be achievable with reasonable drive horsepower.

4.2 30MJ EXPLOSIVE DRIVEN MHD ASSEMBLY

The next requirement addressed was to produce 3000 individual 10 KJ pulses from a set of explosive driven MHD generators powered by a single explosive charge. The pulse required was a half sine wave 700 microseconds in duration. In order to deliver 10 KJ during this pulse, the peak power output per channel is only 20 MW, a level easily achieved using magnetic fields of 2 Tesla.

As discussed in the previous section, the obvious way to increase the chemical energy to electrical energy conversion efficiency is to enlarge the solid angle viewed by the explosive. For this application, a configuration of six generator assemblies facing the charge, as shown in Figure 4.4, was chosen. With a pulse length of 700 microseconds, a channel length of 5 to 6 m appears to be adequate. Slowing down of the detonation products has been observed as energy has been removed, so the average velocity will be much less than the observed initial velocity of 11 Km/sec for the detonation products. One of the areas of greatest uncertainty is how long the detonation products will remain conductive. The 6" x 8" generator experiments reported (5) shows that the generator can conduct current for periods up to about 250 microseconds. The extrapolation of these results by a factor of three in time presents a dilemma, since the exact reason for the seeded detonation products to be so conductive is not

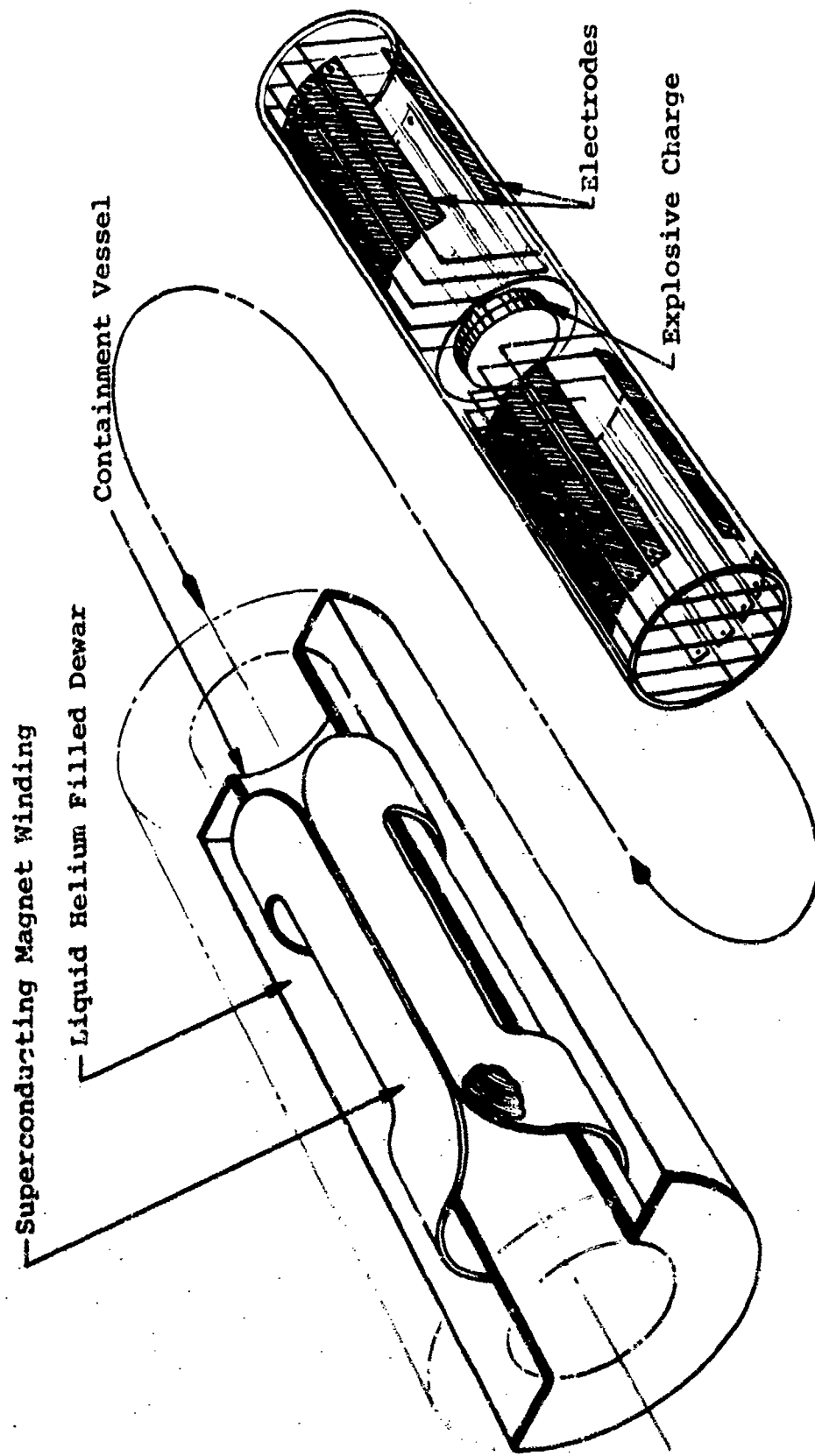


Figure 4.3

DETAILS OF EXPLOSIVE DRIVEN MHD GENERATOR TO
PRODUCE 5MJ PULSES, 100 MICROSECONDS IN DURATION

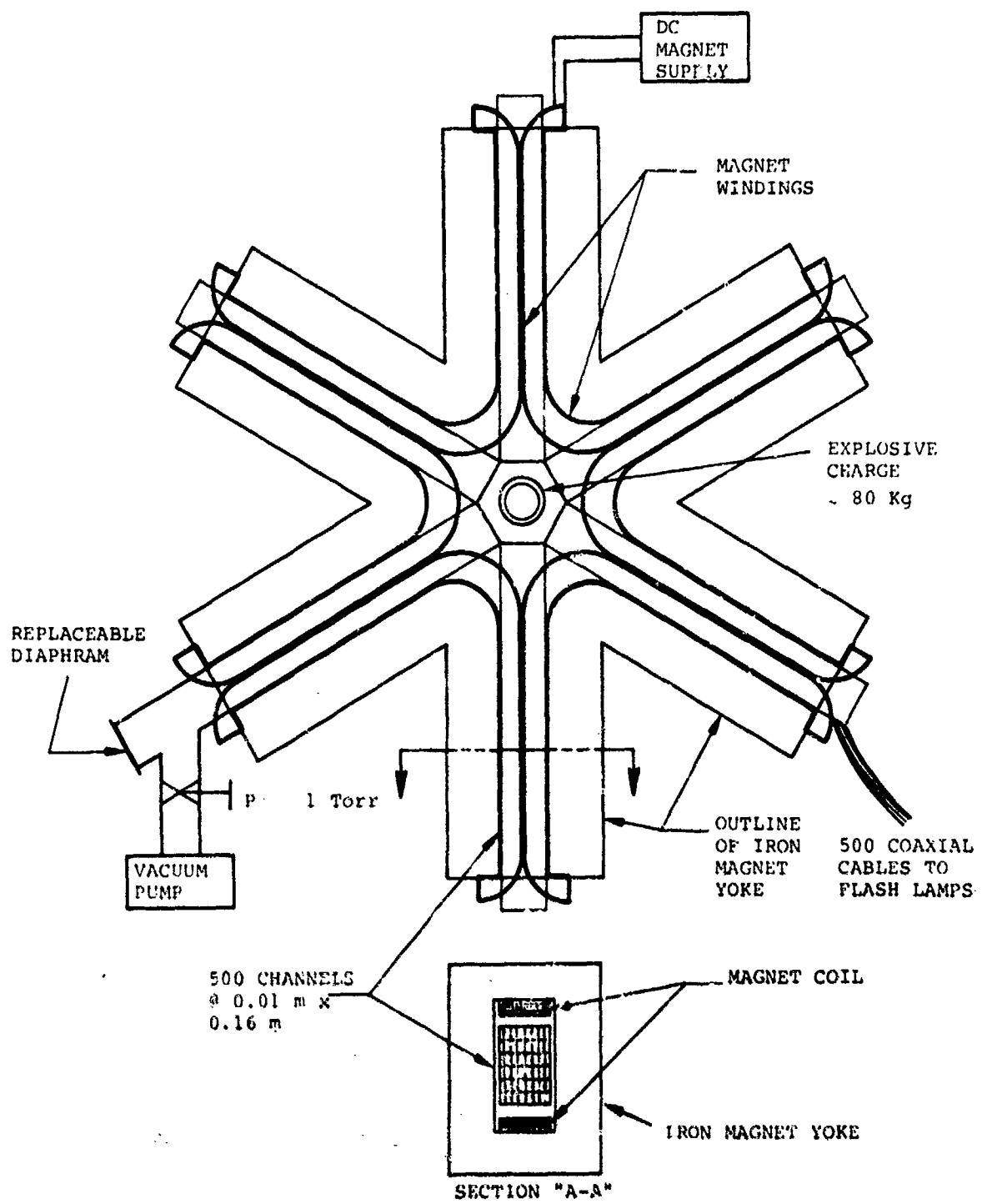


Figure 4.4

CONCEPTUAL DESIGN OF 30MJ EXPLOSIVE
DRIVEN MHD GENERATOR

known with surety in the first place. Experimental verification of conductivity lasting this long, presumably in a simple channel some 4 or 5 meters long, appears to be a matter of high priority for accomplishment.

In order to shape the pulses as a half sine wave, the magnetic induction is lowered at the front part of the channel, the current decay as the plasma level leaves the channel provides the back part of the half sine wave.

The design shown in Figure 4.4 has a plethora of long, high aspect ratio channels. It is anticipated that gas dynamics will probably be the dominant factor determining the pulse trailing edge profile. A more workable solution may be to have the MHD channels a natural size for the magnet, and then have each channel with an internal resistance of about 50 milliohms feed a pulse transformer which would match the driver to 500 of the 20 ohm flash lamps. By using an axially initiated symmetrical charge, timing accuracies of a few percent should be realized between the generators.

This design has a natural advantage that it should be readily scalable up and down in size. Systems-wise, it looks like an inductor which can be discharged on a submillisecond time scale. The size of the pulse essentially scales with the amount of iron and copper in the magnet. Again we repeat that the major area of uncertainty in this design, which could be easily scaled up to 300MJ or more, is the need for experimental confirmation that pulses of this duration can indeed be produced.

4.3 SEEDED DETONATION PRODUCT FAST SWITCH

Another application where explosive driven MHD generator technology appears applicable is in building a repetitively pulsed switch for discharging fast capacitor banks.

The multiple pulse experiments (4) and the alternating current generation experiments (7) have demonstrated the essential elements which are needed to develop a fast switch. In the multiple pulse experiments, a string of charges were sequentially detonated at the entrance to the MHD channel. Pulse rates of up to 100 per second were demonstrated. With the high L/D generator being used, the optimum pulse repetition rate was determined to be 30 per second; however, the experiments demonstrated that charge feed mechanisms could be developed to feed the charges at rates up to 100 per second.

The alternating current generation experiments used a set of segmented electrodes along the MHD generator cross-connected in such a manner that the discrete plasma slug was alternately connected to opposite ends of the load. The experiment produced 20 KHz alternating current at the power level of 2 to 5 MW. The output was subsequently transformed up to the 50 KV level. The important conclusions which may be drawn from this experiment are that the plasma slug has clearly defined front and back boundaries, and that the high pressure (kilobar) detonation products behind the plasma slug have insulating properties which prevented arc-over of the upstream electrodes.

Having seen that surface seeded explosives can produce a carefully controlled slug of highly conductive plasma, and that the unseeded high pressure detonation products following the plasma have good insulation properties, it is logical to propose that seeded detonation products could be used to make a repetitive switch for discharging fast capacitor banks. Typical requirements for such a switch are to pass 1 to 10 coulombs from a 1 MV capacitor in 100 nsec with 100 Hz repetition frequencies. This will require a switch capable of passing 10^7 to 10^8 A, with an internal resistance of less than 1 milliohm.

From these conditions, we can make the following tentative design. To stand-off 1 MV at atmospheric pressure, the gap representing the MHD channel would have to be about 0.35 m (30 KV/cm) high. However, for 10 atm, the gap would only have to be 0.03 m or about 1.3 inches high. Therefore, the use of a pressurized channel appears preferred. To achieve an effective resistance of 1 milliohm, the switch should have an aspect ratio of about 10, which would make a linear switch 13 inches wide for 10 atm, or about 4 inches in diameter if a circular gap is used.

The circular gap has some interesting properties. It can be made as a part of a coaxial conductor system, to minimize inductance, and by adding an axial magnetic field, circulating currents can be developed in the radially expanding plasma ring which will insure that the conductivity is uniform along all segments of the switch. In the radial explosive driven MHD generator experiments (4), a circulating current of 40 ka was measured. With the postulated currents of 10^7 or 10^8 A, the magnetic fields due to the axial current are expected to result in a marked slowing down, and perhaps reversal of the outward plasma flow, which may reduce the requirements for venting the detonation products through the outer

conductor. Under optimum circumstances, it should be possible to have the gap generate 200 kV as an explosive driven MHD generator, overcoming the 100 kV resistive drop in the switch, i.e., 1 milliohm resistance.

The seeded explosive technology required for the circular gap was developed during our work on the radial explosive driven MHD generator (4). The problem of feeding the charges at rates to achieve the desired pulse repetition frequencies are understood, and should not be underestimated. However, these are typically difficult mechanical design problems and it appears that sufficient test work could be conducted on a single pulse basis, to demonstrate the technology before the design of a multiple pulse charge feeding mechanism would have to be undertaken.

From the standpoint of minimizing explosive usage, the coaxial switch appears to be preferred because the switch gap as viewed from the explosive represents a large occluded angle and the coaxial lead assembly should provide a minimum of inductance. In principle, the explosive MHD switch could be placed at the end of the coaxial line which would allow the charges to be easily placed and the detonation products to be conveniently removed. One possible configuration is shown in Figure 4.5.

The basic scale of the switch is set by the gap necessary to hold-off the voltage at atmospheric pressure. The inside radius is determined by the stand-off required from the charge to lower the pressure to workable levels. With small conventional charges detonated at nearly ambient atmospheric pressures, this distance is about 2 or 3 inches. Allowing for a 2 inch diameter charge, the minimum inside diameter of the electrode is about 7 or 8 inches and the outside diameter of the coaxial conductor is 10 to 12 inches for a 100 kV switch. Since the inductance of the coaxial conductor varies as the logarithm of the ratio of the inner and outer conductor diameters, larger diameters may be preferred. Gas vent holes should be provided around the periphery of the outer conductor. High strength magnetic steel blast chambers are shown to back-up the copper electrodes and take a majority of the blast wave impulse load. To avoid arcing at the edges of the gap, a Rogowski electrode contour can be followed.

With this configuration, the feeding of charges is simplified. The biasing magnetic field is provided by a coil powered from a conventional source. Since the purpose of this field is to produce a circulating current in the expanding

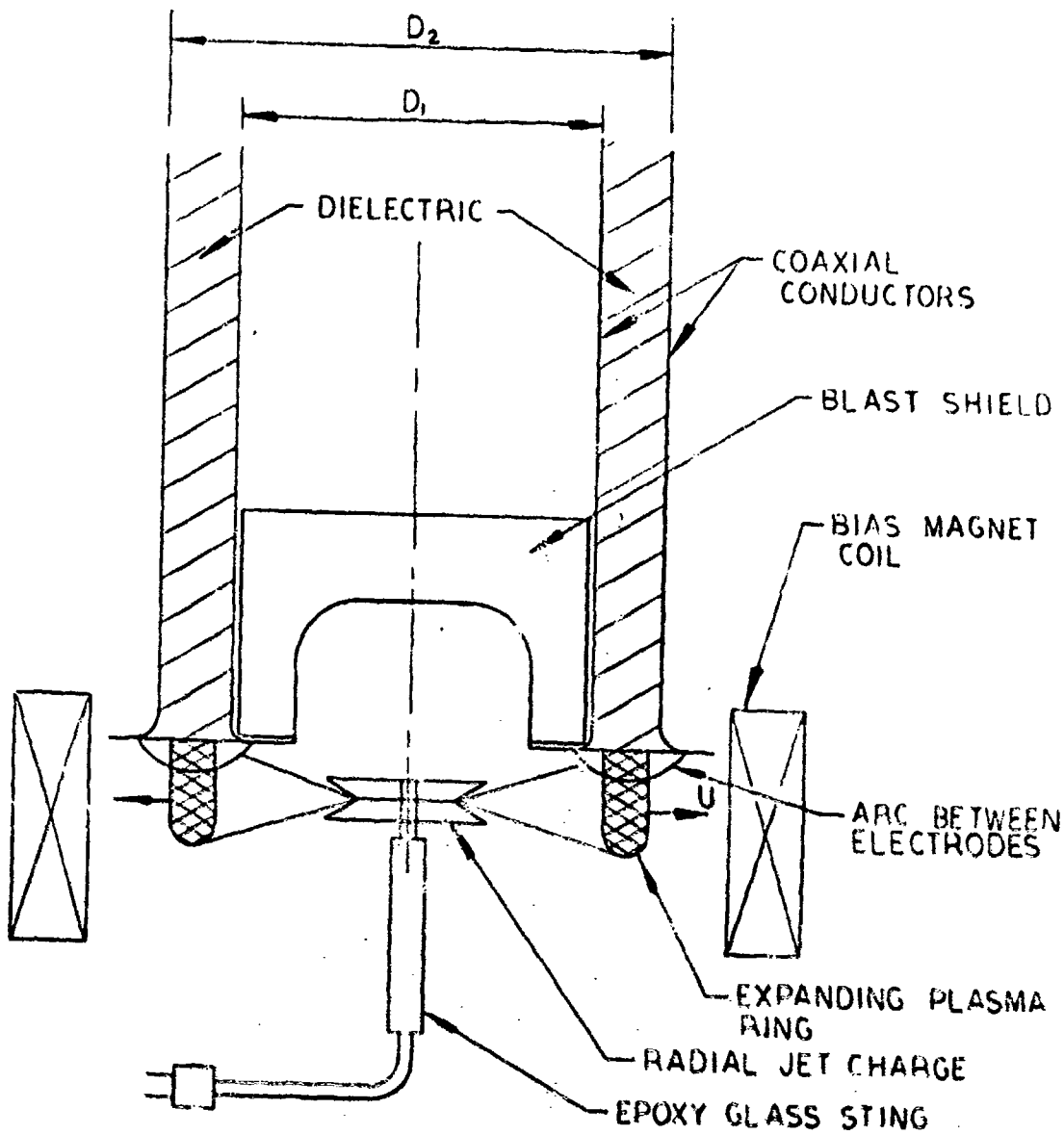


Figure 4.5
EXPLOSIVE MHD SWITCH CONFIGURATION
AT END OF COAXIAL LINE

plasma ring, a fraction of a Tesla should be adequate. One of the key questions is how soon will the gap recover the ability to stand-off high voltages. Figure 4.6 gives the predicted voltage recovery curve for a 1.3 inch gap explosive driven switch. We know with certainty that voltage gradients of 20 kV/m can be maintained within 10 to 25 microseconds. While these results are promising, more data is needed for higher voltages and longer times.

It thus appears that two key experiments are required in order to determine:

1. Can an explosive driven MHD switch pass 10 coulombs in 0.1 microseconds with reasonable voltage drops? And,
2. Can the gap recover to stand-off voltages of 1 Mv within a few 100's of microseconds?

Since these two questions are outside of our previous areas of experimental observation, we can only postulate answers on the basis of our understanding of the physical phenomena. We believe that the answer to the first question is positive. The conductivity is of the proper magnitude and the time scale is about right. The only known problem is that in the linear explosive driven MHD generator experiments, where the time scale is about two orders of magnitude longer, the plasma was shown to have an anomalously high inductance, suggesting that the current had pinched down to a thin filament. We now know, Section 3.1.2, that the seed level plays a dominant role in the apparent high inductance, and that increasing the seed level lowers the effect. For the submicrosecond time scales and high pressures being considered, the dynamics of pinch formation should be too slow to be important.

The answer to the second question should also be positive. We know that the high pressure detonation products are non-conducting. The previously cited experimental evidence implies that there is a high degree of probability that this goal can be achieved.

We conclude that we have every reason to believe that the explosive driven MHD generator concept can be used as a rapid multiple pulse switch for fast capacitor banks. Based on the background data available, it appears feasible to proceed to a direct test of the concept at voltage levels and current levels of interest.

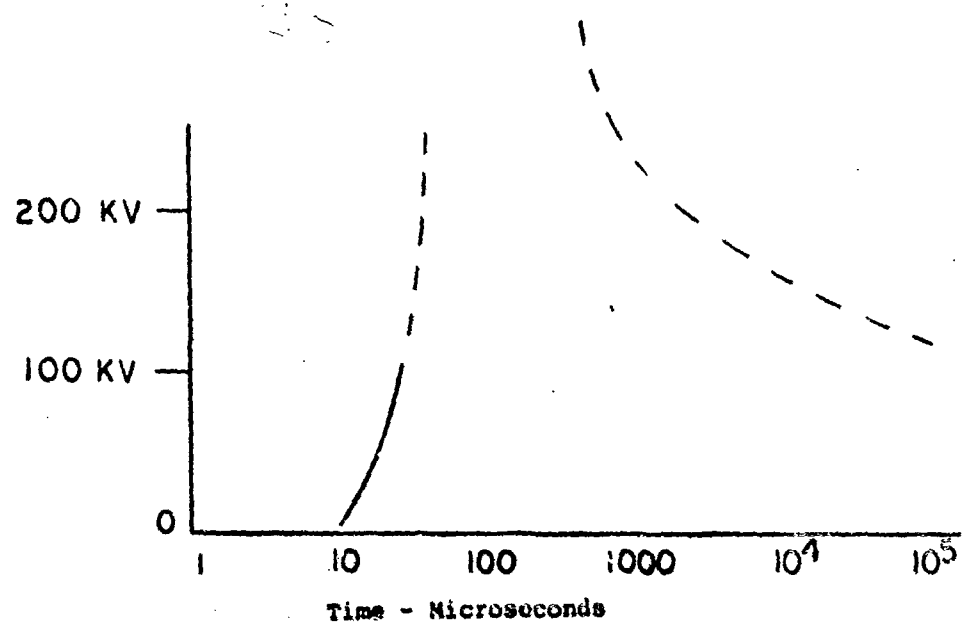


Figure 4.6
PREDICTED VOLTAGE RECOVERY CURVE

4.4 HERCULES SCALE-UP EXPERIMENT

It is believed that much important new data on explosive driven MHD generators could be obtained by constructing a channel which would utilize the full potential of the Air Force owned magnet described in (12). This magnet could be used to scale-up the previous 4" x 6" generator described in (5) to about 12" x 12" (0.3 m x 0.3 m). Since the magnet has an active bore length of about 2 m, a 5 m channel length would allow the investigation of short-circuit pulses out to 600 - 700 microseconds in duration similar to the long electrode generator measurements reported in (4).

The general electrical specifications for the generator would be an open-circuit voltage of about 7000 V, a short-circuit current of about 800 kA, with a peak output of 1.37 GW. With a pulse length of 150 microseconds, this should yield about 200 kJ.

The magnetic energy contained in the generator volume is about 700 kJ, so the output energy could be somewhat higher than the 200 kJ previously calculated.

Based on an explosive loading density of 15 Kg/m³, the charge weight would be 1.35 Kg, which equates to an energy release of 5.8 MJ. A 200 kJ output pulse would represent a 3.4% efficiency for converting chemical energy to electrical energy.

An experiment of this scale would also allow a realistic demonstration of the problems associated with coupling a large group, say twenty, high impedance (20 ohm) lamps to the low impedance pulse generator.

The most valuable data to be gained from the proposed generator test would be definitive proof that pulse lengths in excess of 150 microseconds can be achieved. Obtaining longer pulse lengths is a necessary, but not sufficient, condition for determining whether explosive driven generators can be used for interesting applications. Correspondingly, if there is some reason why longer pulses cannot be obtained, the sooner this can be determined the better it will be for all concerned.

APPENDIX A. ANALYSIS OF WORK PERFORMED UNDER RECENT AIR FORCE CONTRACTS

A.1 AVCO-Shock Hydrodynamics-Atlantic Research Program

The results of the work under this contract are reported in (9).

In general, the report covers a range of system analyses; an investigation of several alternative approaches and a limited amount of experimental data on seeded detonation product conductivity.

A major part of the report is devoted to studies of tubular charges for driving MHD channels. Earlier studies by Burnham, et al, (10), and ourselves (11), had investigated various charge shapes, i.e., conical charges with various angles; W-shaped cone charges; flat front charges, etc. Our conclusions were that shaping the charges could produce a faster current rise time, but that the shape of the charge did not markedly effect the peak power produced. Indeed, because of the larger quantity of explosive used to make the exotic shapes, the ratio of chemical energy input to electrical energy output, i.e., conversion efficiency, usually went down. None of the data presented in Reference (9) indicates that this conclusion should be revised.

The analysis of explosive driven MHD generator systems given in Chapter 3, pp. 83-104, is rather confusing. There are many obvious typographical errors, and evidently some lines of typewritten material were left out which define some of the parameters. One of the major deficiencies of this analysis is that it neglects the circuit inductance, i.e., it assumes a purely resistive load, which is very seldom the case, as is discussed in a later section of that chapter when power conditioning is addressed. However, the time rate of change of internal inductance, L , is implicit in the formulation for the magnetic flux.

We must note that proper application of theory to determine the actual current distribution in the conducting slug would have obviated the need for the elaborate ad hoc assumptions made concerning the "AC skin effect".

We believe that one should resist the urge to convert the equations to a form where the terms which represent the induced magnetic field appear as the magnetic Reynolds number. The generator can be connected in a manner such that the load is at the upstream end and the induced magnetic field does not add to the static magnetic induction. In this case the term $\mu_0 u$ disappears from the analysis and the "magnetic Reynolds number" is no longer explicit in the formulation; however, the physics of the interaction has not changed. While the

equations in the form given in (9) may appear useful for parametric studies, they are not connected directly to measurable quantities which can be controlled. It is much more meaningful to think of the term $\mu_0 u$ as a negative resistance of the order of 10 milliohms per square, which gets compared to the load and plasma resistances per square of channel cross-sectional area; than it is to encumber both parts of this relationship with a σa product which is clouded with a great deal of uncertainty about what is σ , or what is the plasma thickness a , and what is the actual current distribution, etc. The effect of changing the generator electrical connections has been observed directly, magnetic Reynolds numbers can only be implied.

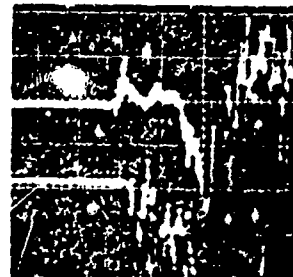
We may note that the discussion of ionization, conductivity and seeding presented on pp. 97-103, made an unreferenced one-line statement about previous explosive derived plasma conductivity measurements and then approached the question of conductivity of seeded detonation products from classical theory of the type used in low pressure/high-density thermal plasmas. That such analyses did not match the experimental data had been known for about ten years. The authors conclude that ". . . no techniques are presently available for accurately calculating the conductivity of explosion products". They then discuss a test program to repeat previous measurements.

The experimental conductivity data reported by this program was extremely limited and is of questionable value.

Analysis of the data does not substantiate the reported results. Figure A.1, which is reproduced from (9), presents an analysis of the data from Test No. 13, for electrodes 99 and 134. For electrode 99, the data shows a current which gradually rises to a level of about 0.4 amperes in 20 microseconds, and then stays about constant, out to the end of the trace. The second trace below that is supposed to show the incremental voltages between probes 5 and 6 for electrode 99. According to the text, these two points are supposedly separated by 20 cm. Reference to the Figure 141, "Sketch of Voltage Probe Locations - Test No. 13" discloses that probe number 5 is at electrode 64 on the top of the channel and probe number 6 is at electrode 134 on the bottom of the channel, and that electrodes 64 and 134 are 14 cm apart, making probes 5 and 6, which are on opposite sides of the 20 cm probe row, actually 22.4 cm apart!



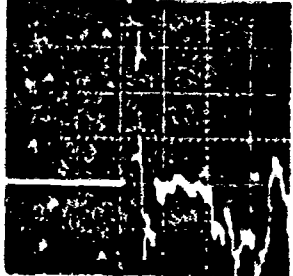
CURRENT - 2V/CM
FOR ELECTRODE 99
VOLTAGE ACROSS 10 OHM RESISTOR



INCREMENTAL VOLTAGE 5-6 2V/CM
FOR ELECTRODE 99
INCREMENTAL VOLTAGE 7-8 1V/CM
ELECTRODE 134



CURRENT - 2V/CM
FOR ELECTRODE 134
VOLTAGE ACROSS 10 OHM RESISTOR



INCREMENTAL VOLTAGE 9-10 2V/CM
FOR ELECTRODE 168

CONDUCTIVITY
TEST NUMBER 13
2-7-73
20 μ s/CM
 $\sigma \approx 750 - 1500$ MHO/METER

FIG. 1e A.1

OSCILLOGRAMS OF TWO SETS OF TRANSVERSE ELECTRODE VOLTAGES
AND CURRENTS FROM AVCO TEST NO. 13
(From pp. 360, Reference (9))

Overlooking such uncertainties, the reference then concludes that for an electric field of 1 to 2 v/m, the "resistance here is $0.5 \text{ ohms} \leq R \leq 1.0 \text{ ohms}$ ". Now the process of injecting 0.4 amperes of current into a plasma from a line electrode on one side, and collecting it with a continuous electrode on the other side, is coupled with a measured electrical field to yield a "resistance" is not clear. The analysis then continues by calculating an electrical cross-sectional area for the current flow, selecting dimensions of "0.002m by 0.16m". The 0.16m dimension is obviously the channel width; however, the source of the 2mm dimension is crucial to a determination of conductivity, absence of the reasoning behind the choice of this dimension makes interpretation of the results uncertain. The reference then goes on to conclude:

1. Gas conductivity at operating pressures of interest in the order of 1000 mhos/m can be achieved.
2. Gas conductivity apparently increases with increasing seed level for 1s to 5s."

Absolutely no analysis of data is presented to substantiate the last claim!

After reviewing the data presented in (9), it is possible to present an alternate interpretation. From the oscilloscope traces representing the current measurements, a precursor wave (presumably a shock wave in the residual air), can be seen propagating down the channel. This is then followed by about a 1m long slug of seeded detonation products moving down the channel with a velocity of 7 to 8 Km/sec. The electrical field distribution in the channel is extremely complex, reaching levels of 50 v/m in localized areas. With three electrodes, 0.07m apart, injecting about 1.5 amperes on one side of the 0.2m high channel, the average current density is of the order of 50 A/m^2 . Using the "measured" electrical field of 2 v/m, this would yield a conductivity of about 25 shos/m, which is of the order of magnitude to be expected for cesium seed material at detonation temperatures.

The amplitude of the current pulses from the various shots is shown in Table A-1, along with the bulk seed levels. It is clear that the 1s and 5s seeded charge detonation products carried more current than the 0.1s seeded charge detonation products. The limited data available does not support the view that the detonation products from the 5s seeded charges is more conductive than from the 1s seed charge.

TABLE A-1. DATA FROM AVCO CONDUCTIVITY TESTS

Shot No.	Seed Level % CS	Current Pulse - Amperes		
		64	99	134
9	0.1	0.25	-	0.28
10	0.1	-	-	-
11	5.0	0.45	-	0.5
12	5.0	> 0.1	-	0.4
13	5.0	> 0.4	0.4	0.6
14	1.0	0.55	0.4	0.6

We conclude that neither of the experimental claims made on page 367 of (9) can be substantiated by the data presented therein.

A.2 The Hercules, Inc., Program

The results of this contract are reported in (11) and (12). Reference (11) covers the analytical studies in detail, while (12) presents the bulk of the experimental data.

A.2.1 Analytical Work on the Hercules, Inc., Program

Central to the analytical development presented in (11) is the conjecture that the gases originally in the channel play a dominant role in determining the characteristics of the generator. The middle of page 3-10 speculates ". . . that mixing of seed and residual gas is the chief source of the conducting zone in the X-MHD generator and the only source if the residual gas does not ionize appreciably. As this is the case, it is of extreme importance that the shocked residual gas temperature be maintained at a level such that adequate conductivity can be achieved."

From this statement, most of the analytical work then proceeds on the basis that the observed 8 Km/sec propagation of the plasma slug defines a shock with a Mach number of 24, which heats the residual gas (at 10 Torr) to 8000°K and compresses it to 10 atmosphere.

This basic assumption about the role of shock heating does not appear to be completely valid on the basis of previous studies which were conducted with residual pressures ranging all the way from 0.03 Torr to atmospheric pressure. Data from studies of this type showed that for pressures less than about 2 Torr, the characteristics of the generator were substantially unchanged, particularly at the low pressure end of the scale. The velocity and conductance appear unchanged. Typical data on generator behavior with changing initial pressures is given in Section 3.1.1. We may, therefore, note that lowering the residual pressure by two orders of magnitude, which in principle increases the shock pressure ratio by two orders of magnitude, thereby increasing the "Mach number" and temperature, does not result in observed changes in the physical parameters. We must, therefore, conclude that the mechanisms postulated by the authors of (11) to explain the operation of explosive driven MHD generators, are probably not valid over the important range of operating variables.

Another key assumption is that the conducting zone has zero thickness. Our earliest work, Figure 2.29 of (1), showed that the conduction zone has considerable axial extent. The alternating current generating experiments described in (7) could only have been possible if the conducting region were about 0.2 m to 0.3 m in length. While this faulty assumption may not be as fatal as the first one, it does have a bearing on major conclusions drawn by the authors relative to pulse rise times.

In addition, we may also note that previous experiments with rapid multiple pulsing, (7), showed that residual explosion products in the channel at near atmospheric pressure, did have a deleterious effect on channel operations for pulse rates greater than 30 per second. The discussion on page 3-14 relative to high repetition rates (100 pps), does not seem compatible with our experimental observations.

Having adopted a shock tube model to explain the linear explosive driven MHD generator, the authors then use such a model to predict channel characteristics. Because of the non-validity of the basic assumptions, we decline to comment on the gas dynamic calculations.

The electrical circuit analyses are presented in Chapter 5. One of the major problems in the analysis presented is that external inductances is largely neglected, and the treatment of induced magnet fields is not handled properly.

The analysis starts by assuming some relationships between shock compression time and current rise time. In most cases of interest, the current rise time is determined by external parameters such as the load inductance, which has been neglected in the analysis. Since the experimental data show that the shock compression time is not a controlling parameter, this analysis is not particularly pertinent.

The next section treats magnetic Reynolds number effects. Equations (1) and (2) are correct, i.e.:

$$R_{m2} = \mu_0 \sigma l \quad (A.1)$$

and

$$\frac{\partial B}{\partial X} = \mu_0 \sigma (uB - v) \quad (A.2)$$

However, the assumption is made that

$$V = \alpha u B_0 h \quad (A.3)$$

where α is the generator loading coefficient, a carryover from open-cycle MHD generator analysis where the induced magnetic fields are small compared to the static magnetic field, and "... B_0 is the magnetic field well ahead of the conducting sheet". This form of analysis has a number of fundamental problems! The concept of using a generator loading coefficient is misleading since α is usually defined in terms of the static magnetic field, B_0 , i.e.,

$$\alpha = \frac{\text{Electric Field Due to Load}}{\text{Open Circuit Electrical Field}} = \frac{V}{h} \cdot \frac{1}{u B_0} \quad (A.4)$$

The error arises in using $\alpha u B_0$ in place of V/h to describe the current density j . The correct treatment of this matter is discussed in Section 3.2 and {13}.

The analysis proceeds to evaluate the constant \bar{B} by introducing the concept that the average of the dynamic magnetic fields, B_1 and B_2 is equal to the static field B_0 . In the process of solving the equations, a minus sign apparently is lost. The proper expression for the magnetic field in this approximation is:

$$B = \frac{2B_0(1-\alpha) \exp(\mu_0 u \alpha (a-x))}{(1+\exp(\mu_0 u \alpha a))} + \alpha B_0 \quad (A.5)$$

which effects the form of both equations (5) and (7) on page 5-5 of {11}. The exponent in the numerator of equation (7) as given in the text is not dimensionally correct.

Reference {11} then examines the question of "circuit rise time", starting on page 5-7. The statement is made that "In a shielded generator, the inductance is mainly that of the conducting sheet itself . . .", without defining what a shielded generator is. Without discussing the significance of the inductance formula, equation (18), which appears to be short two dimensions, and neglecting our previously published work, {4}, which showed that the conducting sheet had a non-negligible self-inductance (60 times the magnitude predicated by equation (8)), the analysis goes on to predict 3 to 7 microseconds rise time. The later experimental work under this program {12}, showed the rise time to be about an order of magnitude larger.

The analysis then continues on page 5-10 to discuss the "well-shielded" generator, with the statement that the time derivative of the internal inductance

is approximately zero, and that for an "unshielded" device, the inductance is a function of x so that there will be a time derivative. What the authors are probably referring to is the generator construction used in the 4" x 6" channel described in (5). Here, one electrode was bonded to the external pressure containment vessel, while the other electrode was supported on an insulating block. Electrically, the pressure containment vessel looks like the outer conductor of a rectangular coaxial cable, with the inner conductor being a rectangular slab displaced toward one of the sides. While the relationship which expresses the inductance per unit length of the coaxial generator, which is of the form $\ln r_1/r_2$, is different than the relationship for the inductance per unit length of the parallel plate generator; there is still an appreciable inductance in the coaxial generator. It, therefore, follows that as the conducting plasma slug shortens the generator length, the inductance will change. Particularly under pulsed conditions where the skin effect may cause the return path through the permeable iron containment vessel to appear to have a higher impedance than the path through the copper electrode, the internal magnetic field distribution of the coaxial generator can approach that of the parallel plate generator. We must, therefore, conclude that the assumption which neglects the time rate of change of the inductance is not justified.

A.2.2 Hercules, Inc., Experimental Results

The results of experiments in back-to-back 0.155 m diameter explosive driven MHD channels are reported in (12). Additional data, which is soon to be published, has been made available for analysis by C. Bangerter. This material includes photographs of oscilloscope traces, test data for all recorded shots and preliminary current and voltage measurements derived from most oscilloscope pictures. Figure A.2 from (12) shows the major details of the experiment. Table A-2 gives a majority of the experimental details for each shot. The terms East and West refer to locations of each channel; East or West of the explosion chamber.

In order to present a clear picture of the basic operation of the generator, we first look at the open-circuit performance of the two generators; then their performance under load, and then summarize their performance on voltage-current diagrams.

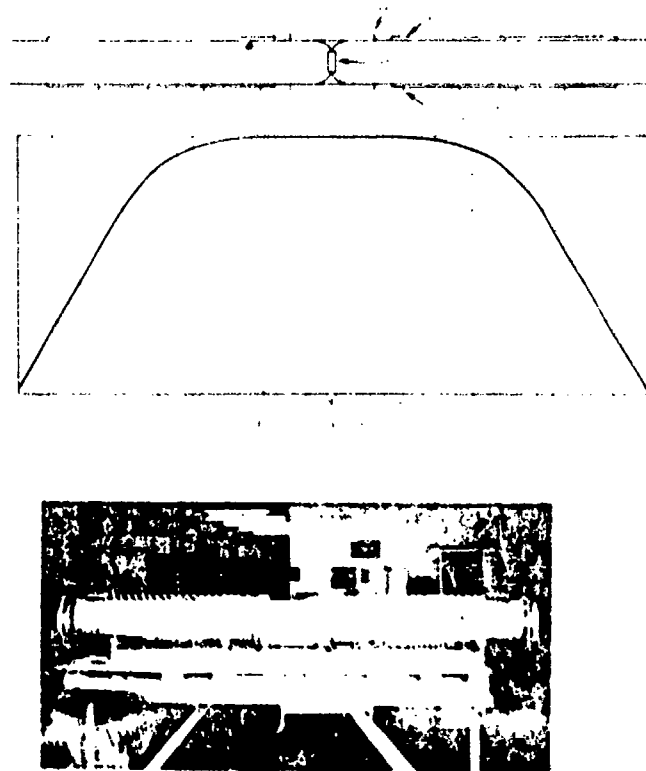


Figure A.2

HERCULES X-MHD CHANNEL SCHEMATIC WITH MAGNETIC FIELD PROFILE AND
PHOTOGRAPH

TABLE A-2
SUMMARY OF HERCULES TEST DATA

Wt. Shot No.	Wt. Charge (g)	Driver Location	Gas	Press. (Torr)	Magnet (kA)	Load E (Ohms)	Load W (Ohms)	Recorded E W	
								I/V	I/V
1	97.3	E	Air	40	11	1k	1k	X	X
2	97.3	E	Air	10	11	975	994	X	X
3	97.3	E	Air	10	11	25m	25m	X	X
4	109	E	Air	10	11	0	0	X	X
5	200	E	Air	10	11	25m	4.89m	X	X
6	100	E	He	5	11	25m	XX	XX	XX
7	100	E	He	650	11	994	975	X	X
8			He	5	11	1000	1000	-	-
9	100	E	He	11	11	994	975	X	X
10	100	W	He	2	11	994	975	X	X
11	100	E	He	2	11	-	-	-	-
12	100	E	He	2.5	9.5	4.89m	4.89m	XX	XX
13	100	E	He	2.5	9.5	0	8.3m	X	XX
14	100	E	He	3.0	9.5	994	8.42m	X	XX
15	100	E	He	2.5	10.5	8.3m	8.22m	XX	XX
16	100	E	He-Ar	3.5	10.5	8.3m	4.89m	XX	XX
17	140	E	He-Ar	3.5	10.5	8.3m	8.22m	XX	XX
18	140	W	He-Ar	280	10.5	8.3m	8.22m	XX	XX
19	109	W	He-Ar	3	10.5	8.3m	8.22m	XX	XX

One fact which emerged from preliminary analysis was that output of the generator was markedly influenced by the presence of the driver used to initiate the main charge. This driver, which usually contained about 5 gms of the explosive PETN in the form of "detasheet", is used to initiate the charge uniformly. This effect is so marked that the data only made sense if we presented it in terms of the "driver" channel and the "driven" channel. In most cases the driver was in the East channel.

A.2.2.1 Open-Circuit Voltage Measurements

The first shot, X-MHD 1, measured open-circuit voltages in both channels. Figure A.3 is the oscilloscope trace for that shot. It is interesting to note that with the driver in the East channel, the voltage came up first on the West, or driven channel, to a value of about 2640 v, while the voltage in the driver channel rose about 5 microseconds later to a value of about 1660 v. We note that the voltage pulse on the driven channel lasted for about 170 microseconds, while the voltage pulse on the driver channel lasted for about 210 microseconds. This implies that there is a connection between pulse shape, length, and induced voltage.

To investigate the influence of the magnetic field profile on the pulse shape, we have attempted to fit the observed pulse shapes from the driver and driven channels with a pulse shape derived from the magnetic field profile, under the assumption that the conducting plasma slug is short in axial extent compared to the field gradient, and that it has uniform velocity. The results of this analysis are shown in Figure A.4. The most clearly defined points are the ends of the electrode, where the voltage starts and stops.

From this detailed analysis of all phases of the pulse, we conclude that the effective velocity in the West channel is about 1.6 times the velocity in the East channel, i.e., the velocity in the West channel is about 5400 Km/sec, and in the East channel, 3300 Km/sec, which is about the same ratio as the open-circuit voltages. A disparity between the channel with the driver and the driven channel, while usually not as large as in this experiment, is noted in all later shots.

Shot X-MHD 2 is another open-circuit experiment, this time at a pressure of 10 Torr of air. The oscilloscope trace is shown in Figure A.5. The peak voltage on the East (driver) channel is 2760 volts and the peak voltage on

Firing No. X-MHD-1 Date June 4, 1974

Charge Specifications:

Composition C-4 Weight: 97.3 gm

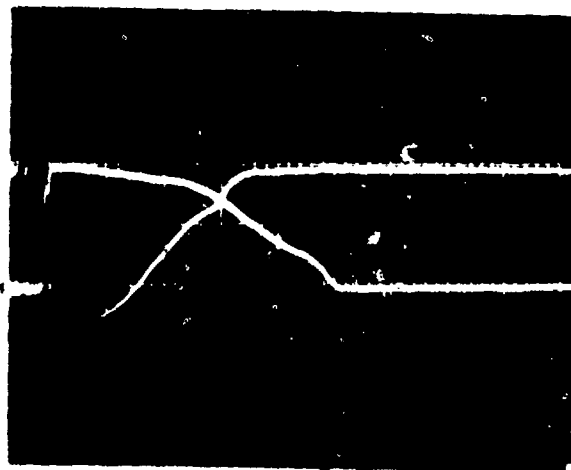
Seed (CsNO₃) Weight: 3.0 gm (bulk)

Standoff Material: 17 gm (west), 21.4 gm (east)

Driver Location: East Channel

Fill Gas: Air Initial Pressure: 40 Torr.

Magnet Current: 11,000 amps.



Upper Trace: West Channel Voltage, 1000 Ω

Vertical Deflection 20 v/cm

Horizontal Deflection 50 μ s/cm

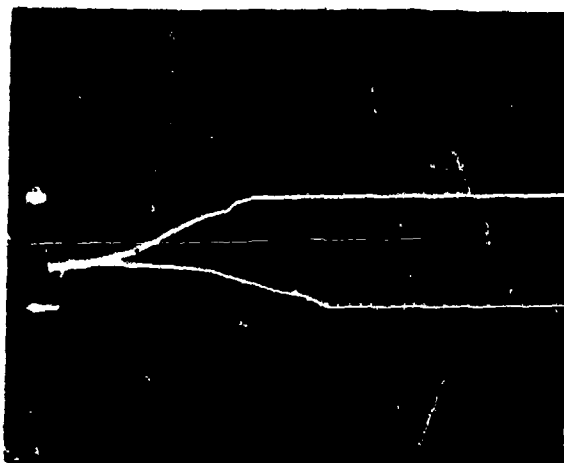
Data Channel *

Lower Trace: East Channel Voltage, 1000 Ω

Vertical Deflection 20 v/cm

Horizontal Deflection 50 μ s/cm

Data Channel *



Upper Trace: West Channel Voltage, 1000 Ω Load

Vertical Deflection 10 v/cm

Horizontal Deflection 50 μ s/cm

Data Channel * (10X attenuation)

Lower Trace: East Channel Voltage, 1000 Ω Load

Vertical Deflection 10 v/cm

Horizontal Deflection 50 μ s/cm

Data Channel * (10X attenuation)

Figure A.3

OSCILLOSCOPE TRACES FOR HERCULES SHOT X-MHD 1

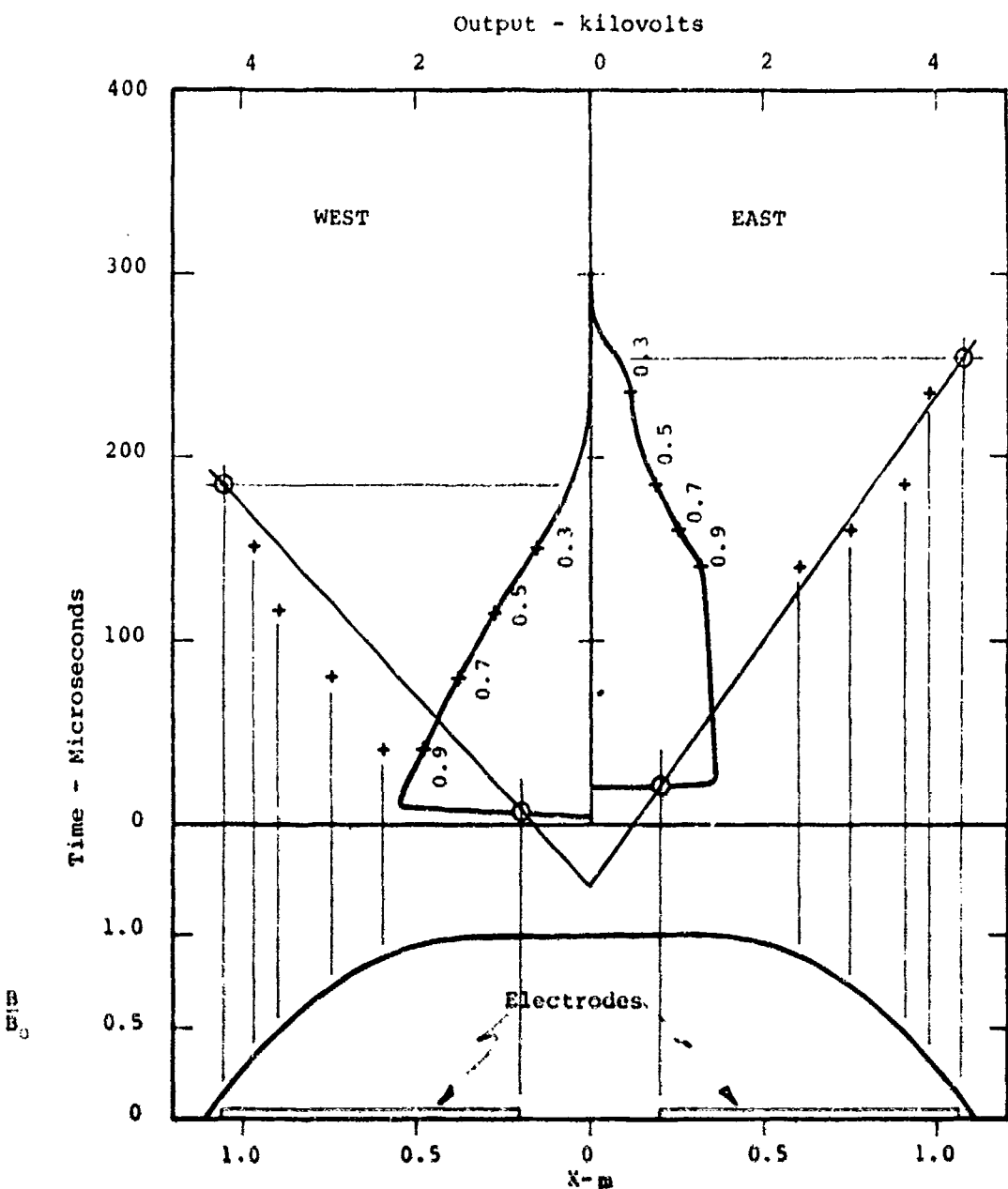


Figure A.4

ANALYSIS OF HERCULES SHOT X-MHD 1.
BOTTON CURVE SHOWS MAGNETIC INDUCTION AND ELECTRODES AS A FUNCTION
OF LENGTH. UPPER FIGURE SHOWS VOLTAGE PULSES ON EAST AND WEST
CHANNELS. CIRCLES SHOW STARTING AND STOPPING OF VOLTAGE. DATA
POINTS ON CURVE REFER TO FRACTION OF PEAK VOLTAGE AND CORRELATION
WITH FRACTION OF PEAK MAGNETIC INDUCTION.

Firing No. X-MID-2

Date June 11, 1974

Charge Specifications:

Composition C-4 Weight: 97.3 gm

Seed (CsNO₃) Weight: 2.7 gm (bulk)

Standoff Material: 12.5 gm each side

Driver Location: East Channel

Fill Gas: Air Initial Pressure: 10 Torr

Magnet Current: 11,000 amps.



Upper Trace: East Channel Voltage, 973 Ω Load

Vertical Deflection 20 v/cm

Horizontal Deflection 10 μs/cm

Data Channel 21

Lower Trace: West Channel Voltage, 994 Ω Load

Vertical Deflection 20 v/cm

Horizontal Deflection 10 μs/cm

Data Channel 21

Figure A.5

OSCILLOSCOPE TRACES FOR HERCULES SHOT X-MID-2

the West (driven) channel is 3150 volts. Comparing the two voltage pulses with the magnetic field profile, similar to the analysis given in Figure A.3, yields a velocity of about 7.25 Km/sec for the driven channel and 6.67 Km/sec for the driver channel.

Figure A.6 is the oscilloscope trace for shot X-MHD 9, which is another open-circuit experiment. The pressure is 11 Torr of a helium-air mixture. The oscilloscope pictures are somewhat confusing. The driven channel voltage pulse, recorded on the top oscilloscope trace, instead of rising sharply, takes almost 80 microseconds to reach the peak, while the East channel has the expected rapid rise, but then shows a negative overshoot at late times. The overshoot is probably due to an internal short which has set-up rather large circulating currents, displacing the ground reference point. The measured peak voltage on the East channel is 2240 V, while the peak voltage on the West was about 2300 V, which occurred at about 100 usec. Because of the "inductive kick" in the East channel trace and the odd shape for the West channel trace, this data will not be considered critically in the overall analysis. This is the sort of electrical breakdown we referred to in Section 2.3 when discussing the selection of gas to initially fill the channel. For shots 1 and 2, the residual gas was air at 10 Torr, for this shot helium with an unknown quantity of leaked-in air.

Shot X-MHD 7 is an open-circuit voltage experiment with 650 Torr of helium in the channel. On the basis of the induced peak voltages, i.e., 2370 volts on the West channel and 2520 volts on the East channel, and the shape of the voltage pulse, which is determined by the magnetic field profile following the procedures used in Figure A.3, we estimate the initial velocity in the West (driven) channel to be about 4.6 Km/sec. The voltage on the East (driver) channel gives an initial velocity of about 4.9 Km/sec. An analysis of the pulse shape is consistent with average velocities of about 4 Km/sec over the pulse length.

This shot has all of the characteristics of an explosive driven helium filled shock tube and its behavior should be well described by the theory presented in (11).

Table A-3 summarizes the open-circuit shots. The average value for B_d derived from this data is 0.56 Tesla-meters, which implies an effective electrode separation of 0.17 m for a magnetic induction of 3.15 Tesla. The actual channel

Firing No. X-MHD-9

Date June 25, 1974

Charge Specifications:

Composition C-4 Weight: 100 gm

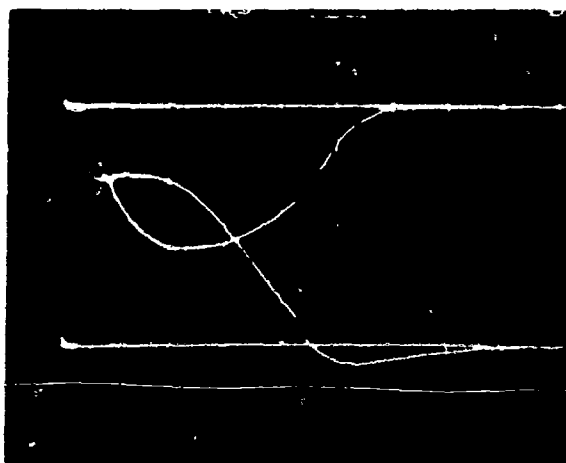
Seed (CsNO_3) Weight: 2.7 gm/side (surface)

Standoff Material: 12.5 gm/side

Driver Location: East Channel

Fill Gas: Helium* Initial Pressure: 11 Torr.

Magnet Current: 11,000 amps.



Upper Trace: West Channel Voltage, 975 μ Load

Vertical Deflection 20 v/cm

Horizontal Deflection 30 μ s/cm

Data Channel 21

Lower Trace: East Channel Voltage, 994 μ Load

Vertical Deflection 20 v/cm

Horizontal Deflection 30 μ s/cm

Data Channel 23

*Leak in channel-gas was probably helium-air mixture.

Figure A.6

OSCILLOSCOPE TRACES FOR HERCULES SHOT X-MHD 9

TABLE A-3

OPEN-CIRCUIT SHOT ANALYSIS

Shot No.	Gas	Pres. (Tors)	Mag. Curr. (kA)	Driver Voltage	Driver Profile Analysis (km/sec)	Driven Voltage	Driven Profile Analysis (km/sec)
1	Air	40	11	2400	3.33	3300	3.65
2	Air	10	11	2760	6.67	3150	7.25
7	He	630	11	2370	3.91	2520	4.19

AVG. $B_d = 0.56$

diameter is 0.155 m, and the minimum separation between electrodes is 0.148 m. The reason for the apparent high effective uBd is not known.

Shot X-MHD 10, which is not reproduced here, was fired with 2 Torr of He in the channel. Again, the "open-circuit" voltage measurements show violent baseline shifts, indicative of extensive internal breakdown. It is again seen that air, which behaves as an electronegative gas because of the electron affinity of O_2 , to form O_2^- , is preferred as an initial filling gas over helium.

In most previous experiments, the effective uBd product has been about 0.8 of the value derived from the product of the separately measured values for each physical quantity. This discrepancy was one reason for suspecting that there were circulating currents in the plasma slug. In addition, the use of a circular channel with the electrodes occupying a 70° segment on each side of the channel should reduce the effective diameter below the geometric diameter because of the circulating currents which must be set-up to keep the electrode surface an equi-potential. The best open-circuit data available, shot X-MHD 2, which had 10 Torr of air in the channel, yields an effective electrode separation of 0.127 m, which is within the expected range.

A.2.2.2. Measurements under Load

The first measurements made with load resistors which approximately match the generator internal resistance were on shot X-MHD 6. The driver channel (East) had a 25 milliohm load, the driven (West) channel, a 4.89 milliohm load. The voltage-current data from the driver channel, Figure A.7, indicates an effective load resistance of 60 to 70 milliohms, much larger than the measured value. (The effective resistances for most loads used in this series of shots was usually much higher than the measured value. The reason for these differences is not clear. It has been speculated that oxide coatings on the connections to the aluminum electrodes may be the cause for the increased resistance.) For some reason the voltage trace for the driven (West) channel went off-scale. The data sheet suggests that the leads might be incorrectly identified. However, since those portions of the voltage traces, which are visible, are coincident with the current pulse for the West channel, and are not coincident with the shorter pulse on the East channel, we conclude that the leads were indeed correctly identified, but that the oscilloscope scale factors are wrong.

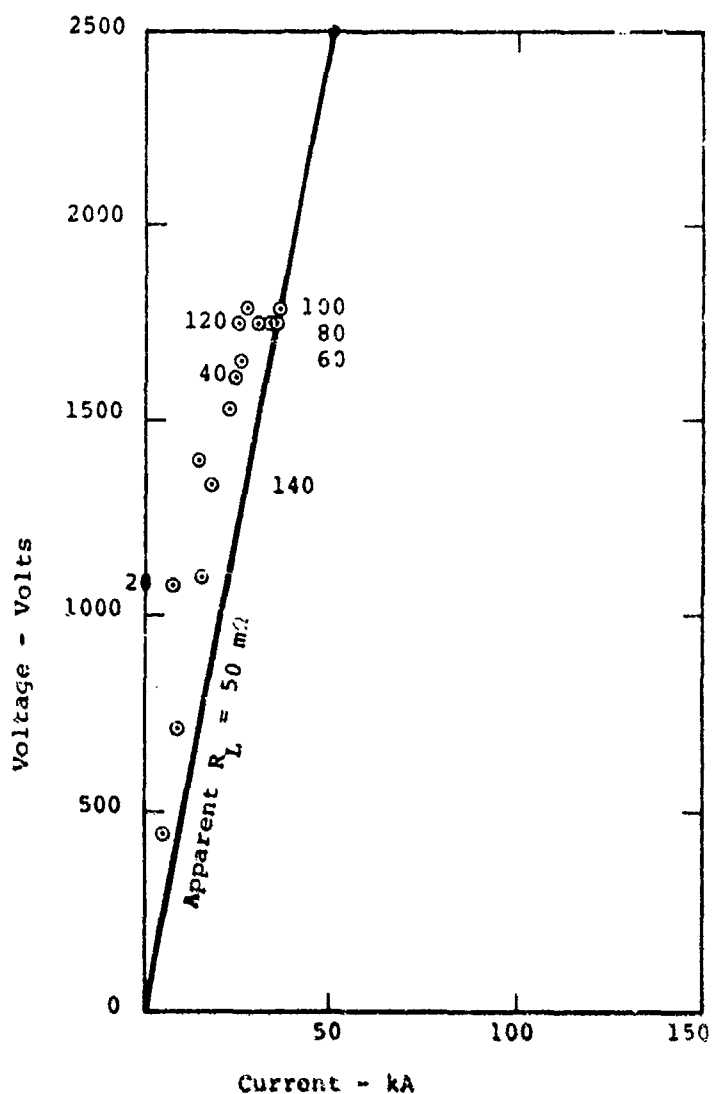


Figure A.7

VOLTAGE-CURRENT PLOT
FOR THE NEST (DRIVEN) CHANNEL
IN HERCULES SHOT X-MHD 6. THE
MEASURED LOAD RESISTANCE WAS 25
MILLIONHMS. THE APPARENT LOAD
RESISTANCE IS ABOUT 50 MILLIONHMS.
NUMBERS BY DATA POINTS REFER TO
TIME IN MICROSECONDS.

The next shot which produced analyzable data was X-MHD 12, which was fired with a lower magnetic field, about 3.15 Tesla, in place of the 3.35 Tesla used in the other experiments. The measured current through the 4.89 milliohms load was 62.4 kA. The voltage trace was on a 4300 V/cm scale, which meant that the deflection was just about trace width (0.2 cm). For comparison purposes, it is estimated that the peak current would have been 70.6 kA, if the magnetic current had been at its nominal value of 11,000 amperes.

For shot X-MHD 13, the data channels appear to be mixed up on the West channel. What is purported to be the current rises rapidly, and then goes negative after the pulse, while what is supposedly the voltage, rises slowly, peaks and then returns to zero. The discrepancy can be seen by plotting the data as a time trajectory on a voltage-current plot. The original data is shown plotted in Figure A.8 as the crosses. In this "trajectory", the current is about 60 kA when the voltage comes on. A more plausible interpretation is to assume the traces were reversed. This analysis produces the trajectory where the data points are shown as circles in Figure A.9. As will be seen from the analysis of other shots, this is the normal trajectory. The apparent load resistance in this interpretation is about 37 milliohms.

Voltage-current trajectories for shots X-MHD 14, 15, 16 and 19 are shown in Figure A.8 through A.11. The apparent load resistance is determined from the measured current and voltage at a time when the current is approximately flat, i.e., $di/dt = 0$. Table A-4 summarizes the observed "load resistances", and provides a comparison with the measured resistance of the load resistor. Since the observed value is determined when $di/dt = 0$, the variance cannot be due to inductive effects, but must be due to contact resistance in the load circuit. The "observed load resistance" is the value which should be used in evaluating the generator power output.

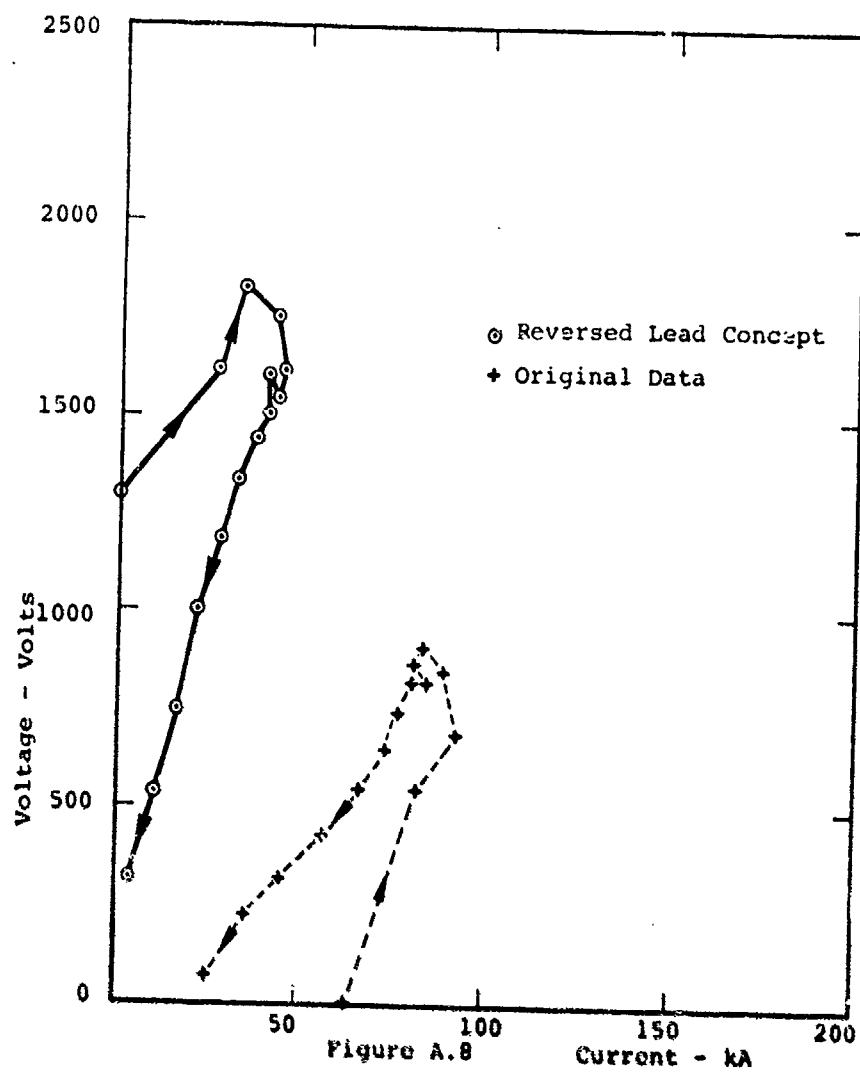
The data from the "Driver" and "driven" channels is shown in Figures A.12 and A.13. The data can be summarized by using a relation of the type:

$$V_g = u_a Bd - IR_{ia}$$

where V_g is the generator terminal voltage when producing a current I through an external load, B is the static magnetic induction, d , the electrode separation, R_{ia} and u_a are the internal generator resistances and effective gas

TABLE A-4
EFFECT LOAD RESISTANCES - MILLIOHMS

Shot No.	E	R _L		Apparent R _L	
		W	E	W	E
6	25	-	50	-	-
12	4.89	4.89	1.5	-	-
13	0	8.3	-	37	-
14	994	8.42	-	9.0	-
15	8.3	8.22	49	10.4	-
16	8.42	4.89	33	6.8	-
17	8.3	8.22	-	-	-
18	8.3	8.22	-	-	-
19	8.3	8.22	23	12.5	-



VOLTAGE-CURRENT TRAJECTORIES FOR THE WEST CHANNEL
IN SHOT X-MUD 11. LOAD IS 8.1 MILLIONH. CROSSES
SHOW DATA AS PRESENTED IN DATA SHEETS. DATA POINTS
ARE 10 MICROSECONDS APART. CIRCLES, WHICH SHOW
ALTERNATE INTERPRETATION THAT INSTRUMENTATION LEADS
WERE CROSSED, FOLLOWS NORMAL TIME TRAJECTORY. SEE
FIGURE A.9.

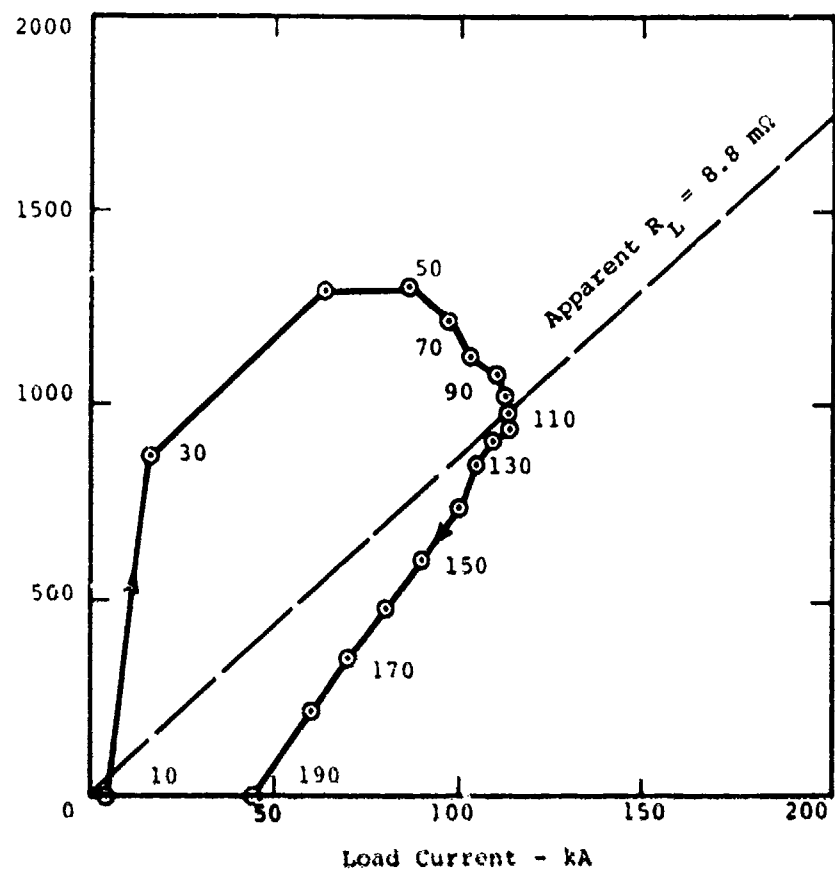


Figure A.9

VOLTAGE-CURRENT TRAJECTORIES FOR THE WEST CHANNEL
ON HERCULES SHOT X-MHD 14. LOAD MEASURED AS 8.42
MILLIOHMS. NUMBERS BY DATA POINTS REFER TO TIME
IN MICROSECONDS.

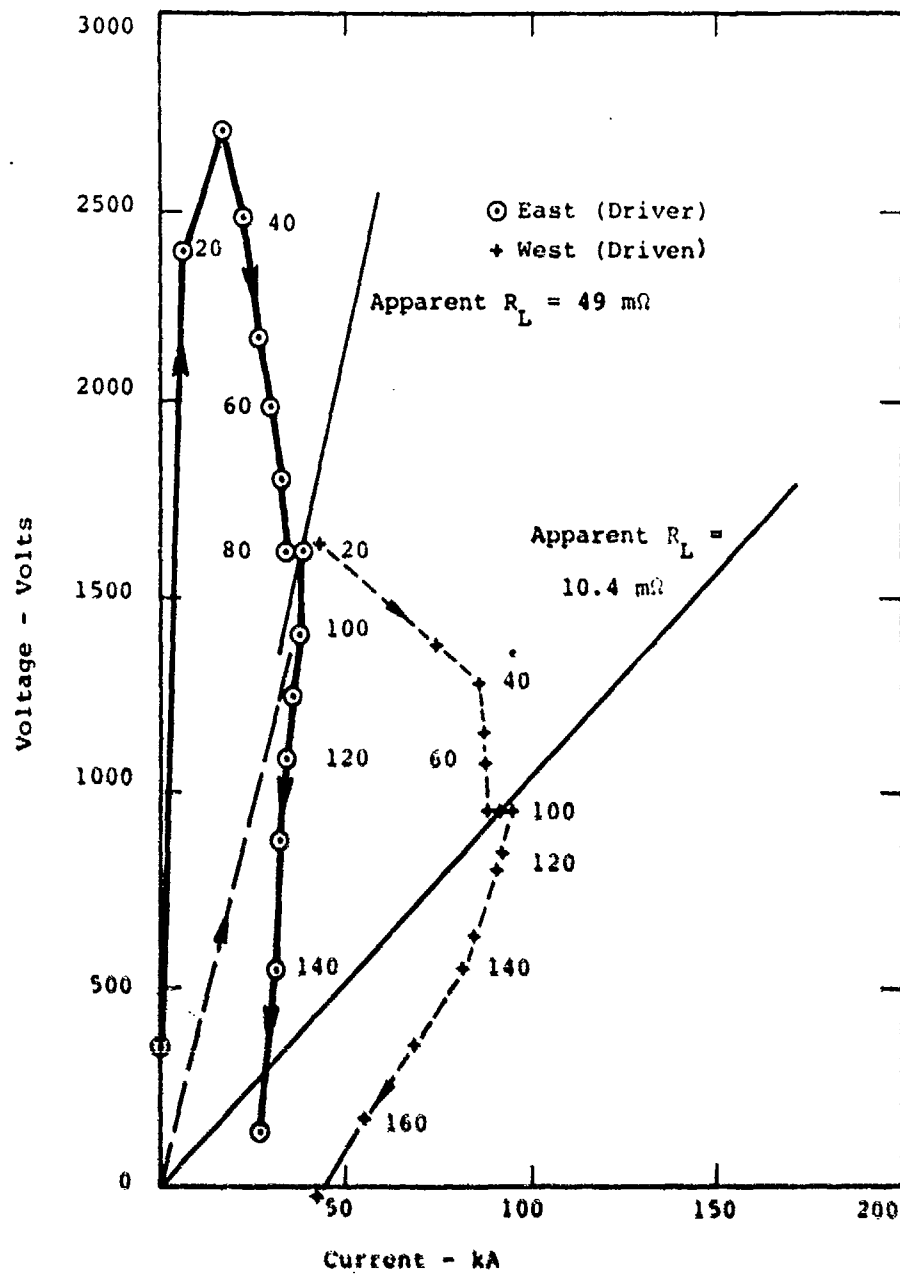


Figure A.10

VOLTAGE-CURRENT TRAJECTORIES FOR HERCULES
SHOT X-NHD 15. LOAD ON EAST CHANNEL IS
8.3 mΩ. LOAD ON WEST CHANNEL IS 8.22 mΩ.
NUMBERS BY DATA POINTS REFER TO TIME IN
MICROSECONDS.

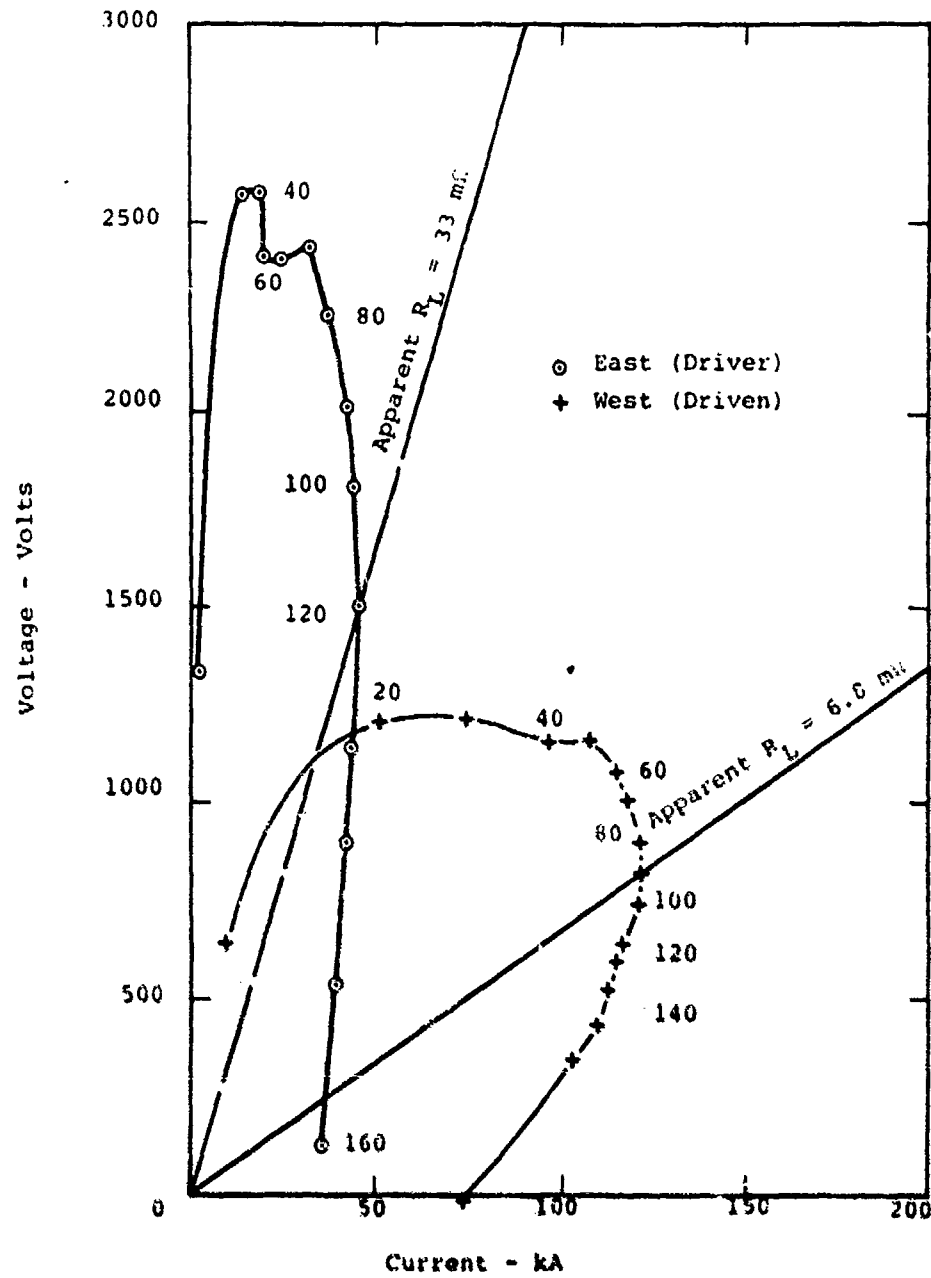


FIGURE A.11

CURRENT-VOLTAGE TRAJECTORY FOR HERRINGSHOT
SHOT X-NID 16. LOADS WERE 8.42 mΩ ON
EAST CHANNEL AND 4.89 mΩ ON WEST CHANNEL.
NUMBERS BY DATA POINTS REFER TO TIME IN
MICROSECONDS.

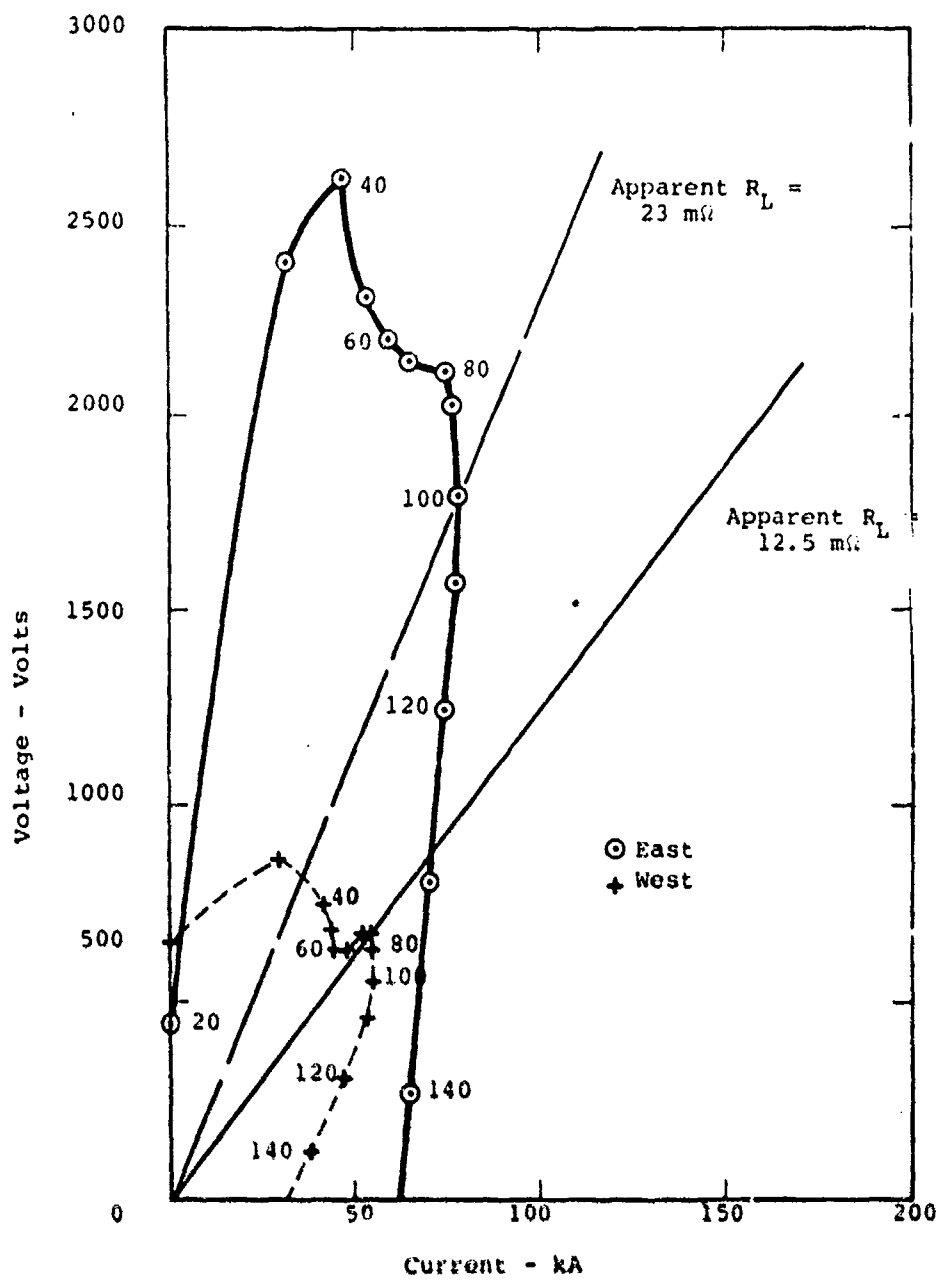


Figure A.12

VOLTAGE-CURRENT TRAJECTORIES FOR HERCULES SHOT X-MHD 19. LOAD RESISTANCES WERE $8.2 \text{ m}\Omega$ ON THE WEST CHANNEL AND $8.3 \text{ m}\Omega$ ON THE EAST. NUMBERS BY THE DATA POINTS REFER TO THE TIME IN MICROSECONDS.

velocities determined from the data in Figures A.12 and A.13. Using the subscript r for the driver channel and the subscript n for the driven channel, we have:

$$V_r = 5224 Bd - 0.033 I$$

$$V_n = 6157 Bd - 0.021 I$$

The authors of (12) recognize the problem and address various ways of initiating the charge in a manner such that the detonation products from the initiating system are not injected into the channel ahead of the seeded detonation products.

From Figures A.12 and A.13, it appears that the peak power output of the driven generator can be about 129 MW, and the driver generator about 60 MW. This means that the maximum output of the driver generator can only be less than 1/2 of the driven generator.

Table II of (12) shows a maximum output of the driven generator of 11.8 kJ for test X-MHD 14. In this test, the driver channel was open-circuited, whereas, the abstract states that ". . . due to magnetic field non-uniformity and asymmetric drive of the two channels, it produced 18 kilojoules. Two thirds of this was produced in the channel which was properly driven." Nowhere in Table II is there any data which shows more than 11.8 kJ being produced. In shot X-MHD 16, only 10.55 kJ were produced between the two channels. In shot X-MHD 15, 9.17 kJ. We have examined the effects of the asymmetric drive and agree with the conclusion that if both channels had been hooked to appropriate loads the generator could have produced 18 kJ; however, the fact is that it did not:

The abstract of (12) then goes on to state, "Calculations which correct for these two conditions predict an efficiency of 8% would have been obtained . . .". Allowing for 5% additional explosive to be used in the plane wave generator, the conversion efficiency of shot X-MHD 14 actually was about 2.7%. Assuming that the other channel had been connected to the optimum load to deliver an additional 5.5 kJ, as indicated by the relations discussed above, the overall efficiency would have been 3.5%. If we further assume that both channels could put out 11.8 kJ, the conversion efficiency would still be only about 5%, and not the 8% cited in the abstract!

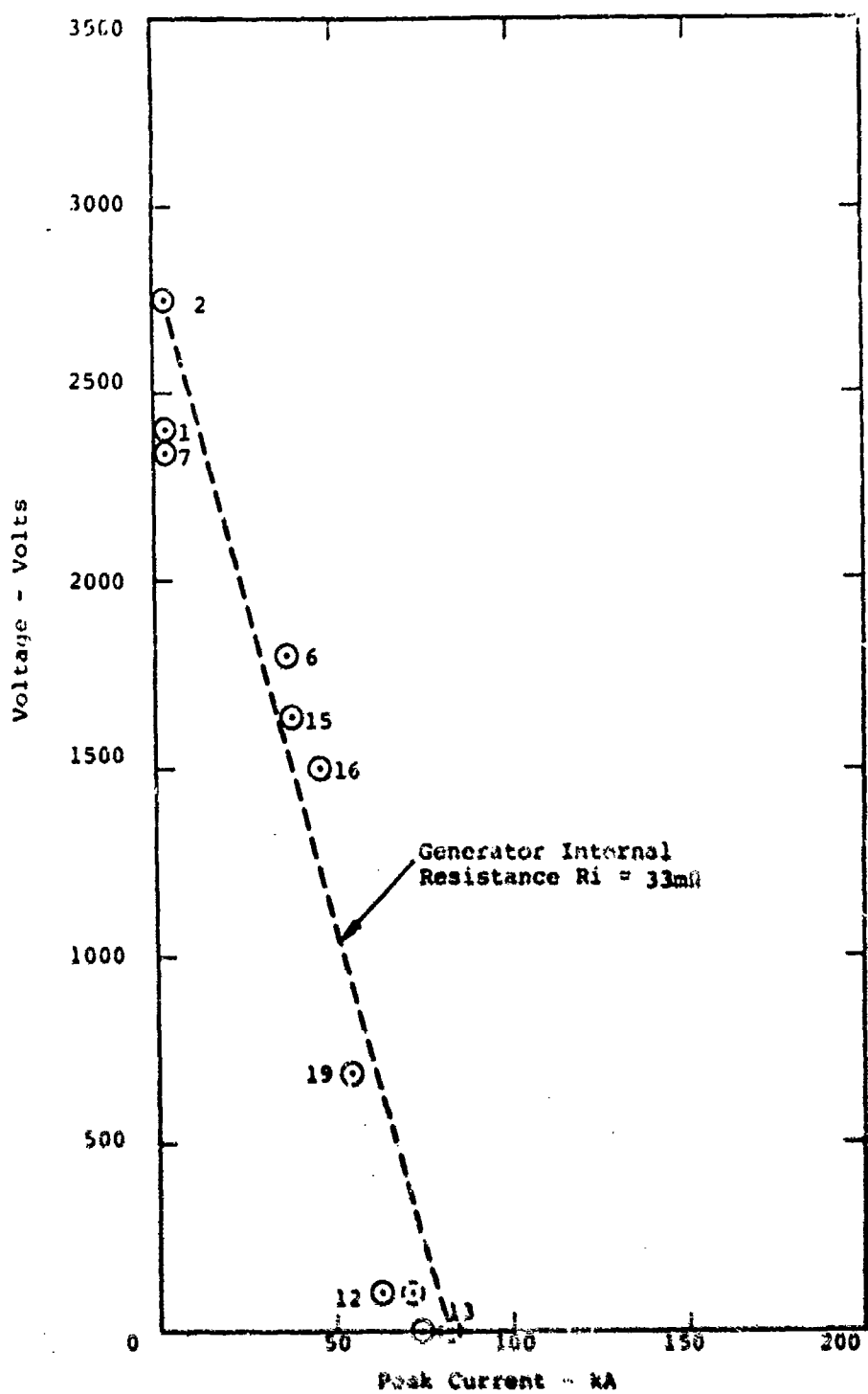


Figure A.13

SUMMARY OF PEAK CURRENT DATA FOR THE DRIVER CHANNEL IN THE HERCULES EXPERIMENTS. NUMBERS BY THE DATA POINTS REFER TO THE SHOT NUMBER. DATA FOR SHOT X-MID 1 IS BASED ON THE HIGHER OF THE SCALE FACTORS DERIVED FROM FIGURE A.3. GENERATOR APPARENT INTERNAL RESISTANCE IS $33 \text{ m}\Omega$.

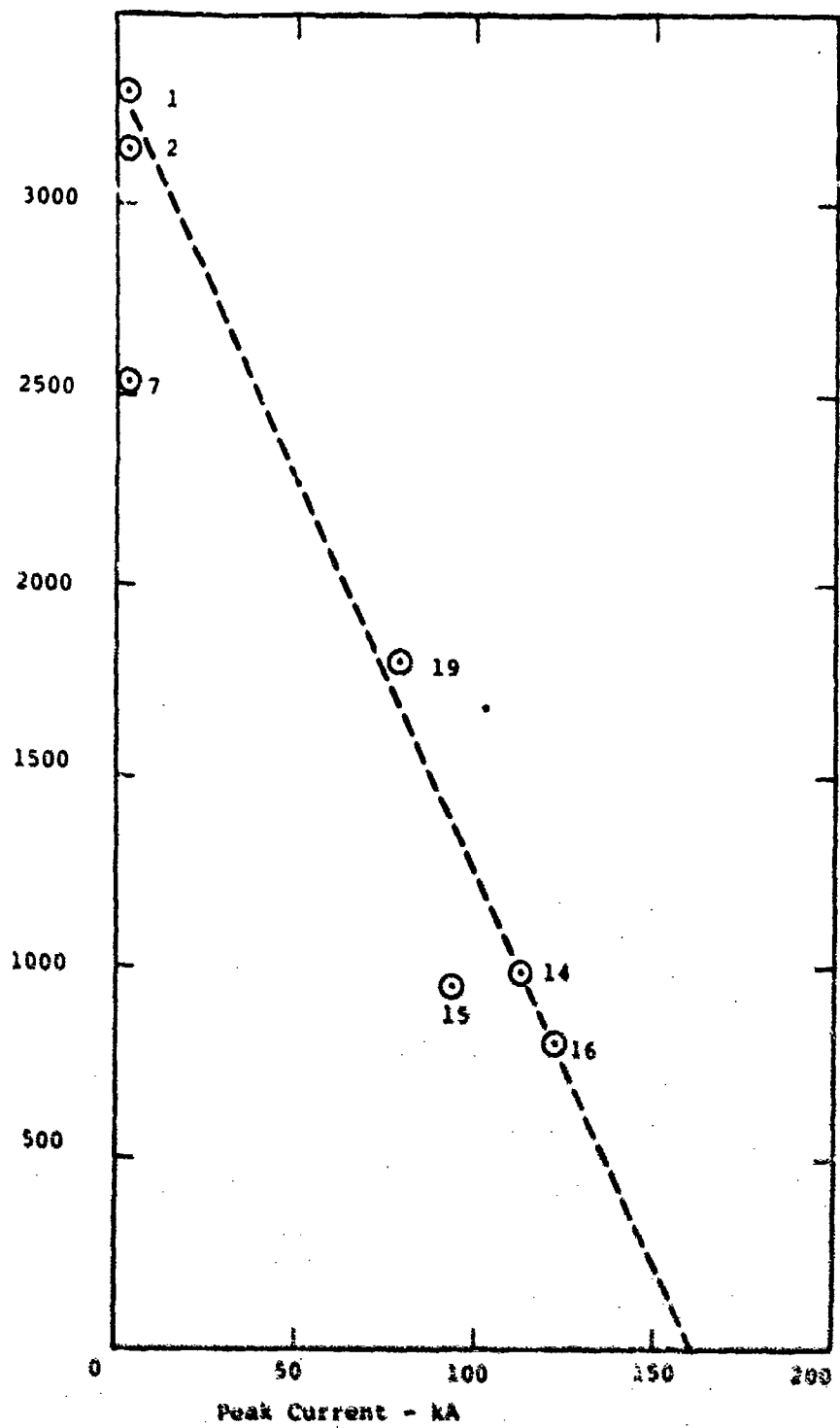


Figure A.14

SUMMARY OF PEAK CURRENT DATA FOR THE DRIVEN CHANNEL IN THE HERCULES EXPERIMENTS. NUMBERS BY THE DATA POINTS REFER TO THE SHOT NUMBER. DATA FOR SHOT NO. X-NHD 1 BASED ON THE HIGHER OF THE SCALE FACTORS DERIVED FROM FIGURE A.3. GENERATOR APPARENT INTERNAL RESISTANCE IS 31 MILLIONMS.

The question of magnetic field non-uniformity is never discussed in the text. With a magnet of the size shown in Figure 14 of (12), the field should be substantially uniform over the 0.155 m channel diameter. What the authors probably refer to is the fact that the magnetic induction has fallen off to negligible values after the plasma has traveled about 0.8 m; see Figure A . . This was inherent in the design of the experiment. One usually does not have a strong MHD interaction if the magnetic field vanishes. It is true that if they had a longer magnet they probably could have produced longer pulses and converted more of the chemical input energy to electrical energy in their load. but they did not. While on this topic, we should note that in (12) near the top of page 6, the authors discuss pulse lengths and claim, "Reasonably flat topped pulse durations of 20-400 microseconds are attainable . . .", and then conclude this paragraph with the statement, "Longer flat top pulse duration will probably require tailoring of explosive characteristics and for channel area contouring which probably can extend pulse duration to 750-1000 microseconds at tolerable loading." The experimental data presented in (12) neither supports nor contradicts these claims. As we have previously stated in Chapter 4, experimental demonstration of long duration explosive driven MHD generator pulses is a key milestone in developing explosive MHD technology for useful applications.

We conclude that the Hercules, Inc., program has made a valuable contribution to the explosive driven MHD generator technology. It has demonstrated the operation of back-to-back channels facing a single explosive charge, a concept which was proposed independently in (7). It has also shown that by going to the lower explosive loading density of 5.29 kg/m³, compared to the 15 kg/m³ used for the tests reported in (9), and by increasing the magnetic induction from 2.8 Tesla to 3.35 Tesla, that the chemical to electrical conversion efficiency can be improved.

UNCLASSIFIED

SECURITY CLASSIFICATION OF THIS PAGE (When Entered)

REPORT DOCUMENTATION PAGE

READ INSTRUCTIONS
BEFORE COMPLETING FORM
REF ID: A6525

1. REPORT NUMBER	2. GOVT ACCESSION NO.	3. RECIPIENT'S CATALOG NUMBER
4. TITLE (and Subtitle) FUNDAMENTAL RESEARCH IN EXPLOSIVE MAGNETOHYDRODYNAMICS		5. TYPE OF REPORT & PERIOD COVERED FINAL 1 Oct 74 - 31 Dec 75
6. AUTHOR(s) MALCOLM S JONES, JR		7. CONTRACT OR GRANT NUMBER(s) F44620-75-C-0017
8. PERFORMING ORGANIZATION NAME AND ADDRESS MALCOLM JONES ASSOCIATES, INC POST OFFICE BOX 67 CORONA DEL MAR, CALIFORNIA 92625		9. PROGRAM ELEMENT, PROJECT, TASK AREA & WORK UNIT NUMBERS 681308 9752-02 61102F
10. CONTROLLING OFFICE NAME AND ADDRESS AIR FORCE OFFICE OF SCIENTIFIC RESEARCH/NA BUILDING 410 BOLLING AIR FORCE BASE, D C 20332		11. REPORT DATE Feb 76
12. MONITORING AGENCY NAME & ADDRESS (if different from Controlling Office)		13. NUMBER OF PAGES 77
		14. SECURITY CLASS. (of this report) UNCLASSIFIED

15. APPROVAL STATEMENT (for this Report)

Approved for public release; distribution unlimited.

16. DISTRIBUTION STATEMENT (for the abstract entered in Block 20, if different from Sec 14)

17. SUPPLEMENTARY NOTES

18. KEY WORDS (check one or more of the boxes and submit by block numbers)

EXPLOSIVE DRIVEN NID GENERATORS **T-LAYERS**
CONDUCTIVITY OF SEDDED DTONATION PRODUCTS
PLASMA DISSOCIATION EFFECT
CIRCULATING CURRENTS
BULK SEDDED AND SURFACE SEDDED EXPLOSIVES

This report reviews the physical parameters involved in the design of explosive driven NID generators, and presents previously unpublished experimental data on the effects of the gases originally in the channel on generator performance, and experiments which compare bulk seeding of the explosive charge with surface seeding. It is concluded that the seeding level controls not only the plasma conductance, but the plasma slug inductance as well. Several mechanisms which may be responsible for the observed plasma conductivity are examined. It is concluded that circulating currents due to velocity gradients or magnetic field

UNCLASSIFIED

SECURITY CLASSIFICATION OF THIS PAGE (What, Date Entered)

gradients are of the magnitude necessary, when in a magnetic field, to initiate a thermal instability phenomenon described as "T-layers" in the plasma. While this mechanism is adequate to describe the maintenance of the conductivity, it does not explain the conductivity observed in the absence of a magnetic field in the seeded detonation products near the explosion. To identify key problem areas, several scaled-up MHD generator designs are examined, as well as the prospect of using explosive driven MHD generator technology as a switch for discharging fast capacitor banks. The major unresolved question is what is the maximum pulse duration that can be achieved in explosive driven MHD generators. Recent experimental work, which is reviewed, does not extend time durations beyond previously observed times of several hundred microseconds; however, the circulating current models described above predict that pulse times of the order of 1 millisecond can be achieved.

REFERENCES

- (1) Jones, M. S., Blackman, V. H., Brumfield, R. C., Evans, E. W., and McKinnon, C. N., Research on the Physics of Pulsed MHD Generators, Final Report Contract, Nonr 3859(00), AD 426 448, December 1963.
- (2) Jones, M. S., McKinnon, C. N., and Blackman, V. H., "Generation of Short Duration Pulses in Linear MHD Generators," Fifth Symposium on Engineering Aspects of Magnetohydrodynamics, April 1964, Massachusetts Institute of Technology.
- (3) Jones, M. S. and Blackman, V. H., "Parametric Studies of Explosive Driven MHD Generators." MHD Electrical Power Generation, Proceedings of an International Symposium, Vol. 2, Paris (1964).
- (4) Jones, M. S., Explosive Magnetohydrodynamics, AFAPL-TR-65-61, AD 470 711, April 1965.
- (5) Jones, M. S., Peterson, A. H., and Church, C. H., Explosive Driven MHD Generators for Laser Pumping, AFAL-TR-65-256, November 1965.
- (6) Jones, M. S. and McKinnon, C. M., "Explosive Driven Linear MHD Generators," Proceedings of the Conference on Megagauss Magnetic Field Generation by Explosives and Related Experiments, Frascati, Italy, September 21-23, 1965.
- (7) Jones, M. S., Bangerter, C. D., Peterson, A. H., and McKinnon, C. N., Explosive Magnetohydrodynamics, AFAPL-TR-67-64, August 1967.
- (8) Jones, M. S., "Experimental Observation of a Peak Current Limit in Explosive Driven MHD Generators." 13th Symposium on Engineering Aspects of Magnetohydrodynamics, March 1973, Stanford University.
- (9) Teno, J. and Sonju, O. K., Development of Explosively Driven MHD Generator for Short Pulse Aircraft High Power, AFAPL-TR-74-48, AD 784903.
- (10) Burnham, M. W., Marshall, S. J., Krill, A. M., "The Influence of a Curved Duct on Explosive Driven MHD Converters," MHD Electrical Power Generation, Proceedings of an International Symposium, SM 74/173, Salzburg (1966).
- (11) Bangerter, C. D., et al, Explosive Magnetohydrodynamic Program, AFAPL-TR-73-16, May 1973.
- (12) Bangerter, C. D., et al, "Explosively Driven Power Generation: A Progress Report," Sixth International Conference on Magnetohydrodynamic Electrical Power Generation, Vol. IV, Washington, DC, June 1975.
- (13) Sinkevich, O. A., Krylova, L. M., "Plasma Slug Motion in Channel with Variable Inductance, Magnitnaya Gidrodynamika, Vol. 6, No. 1, pp. 28-34, 1970.
- (14) Asinovskii, E. I., Kuznetsov, Yu. A., Lebedev, E. F., Maximov, A. M., Ostatshov, V. E., "The Movement of Plasma Pushed by a non Conductive Piston in a Magnetic Field," Sixth International Conference on Magnetohydrodynamic Electrical Power Generation, Vol. IV, Washington, DC, June 1975.
- (15) Alexeev, V. A., Velikov, E. P., and Lopancheva, G. B., "The Conductivity of a High Density Plasma," MHD Electrical Power Generation, Proceedings of an International Symposium, SM-74/102, Salzburg (1966). Also see High Temperature Journal, 1970.
- (16) Kulik, Journal of Experimental and Theoretical Physics, USSR, December 1971.
- (17) Kirillin, V. A., Schendlin, A. E., et al, "Impulse Magnetohydrodynamic Generator with Superconducting Magnet System," Technical Physics, Academy of Natural Sciences, USSR, Doklady, 177, No. 1, 77 (1967).
- (18) Roberts, A. S. Jr., and Palmgren, S., "Pulsed MHD Generator Analysis with High Induced Fields," Eleventh Symposium on Engineering Aspects of Magnetohydrodynamics, March 1970, California Institute of Technology.